Journal of Inflammation

RESEARCH

Open Access

Anti-hyperalgesic and anti-inflammatory effects of 4R-tobacco cembranoid in a mouse model of inflammatory pain

Luis G. Rivera-García[1,2], Adela M. Francis-Malavé[1], Zachary W. Castillo[3], Calvin D. Uong[3], Torri D. Wilson[1], P. A. Ferchmin[2], Vesna Eterovic[2], Michael D. Burton[3] and Yarimar Carrasquillo[1,4*]

Abstract

4R is a tobacco cembranoid that binds to and modulates cholinergic receptors and exhibits neuroprotective and anti-inflammatory activity. Given the established function of the cholinergic system in pain and inflammation, we propose that 4R is also analgesic. Here, we tested the hypothesis that systemic 4R treatment decreases pain-related behaviors and peripheral inflammation via modulation of the alpha 7 nicotinic acetylcholine receptors (α7 nAChRs) in a mouse model of inflammatory pain. We elicited inflammation by injecting Complete Freund's Adjuvant (CFA) into the hind paw of male and female mice. We then assessed inflammation-induced hypersensitivity to cold, heat, and tactile stimulation using the Acetone, Hargreaves, and von Frey tests, respectively, before and at different time points (2.5 h – 8d) after a single systemic 4R (or vehicle) administration. We evaluated the contribution of α7 nAChRs 4R-mediated analgesia by pre-treating mice with a selective antagonist of α7 nAChRs followed by 4R (or vehicle) administration prior to behavioral tests. We assessed CFA-induced paw edema and inflammation by measuring paw thickness and quantifying immune cell infiltration in the injected hind paw using hematoxylin and eosin staining. Lastly, we performed immunohistochemical and flow cytometric analyses of paw skin in α7 nAChR-cre::Ai9 mice to measure the expression of α7 nAChRs on immune subsets. Our experiments show that systemic administration of 4R decreases inflammation-induced peripheral hypersensitivity in male and female mice and inflammation-induced paw edema in male but not female mice. Notably, 4R-mediated analgesia and anti-inflammatory effects lasted up to 8d after a single systemic administration on day 1. Pretreatment with an α7 nAChR-selective antagonist prevented 4R-mediated analgesia and anti-inflammatory effects, demonstrating that 4R effects are via modulation of α7 nAChRs. We further show that a subset of immune cells in the hind paw expresses α7 nAChRs. However, the number of α7 nAChR-expressing immune cells is unaltered by CFA or 4R treatment, suggesting that 4R effects are independent of α7 nAChR-expressing immune cells. Together, our findings identify a novel function of the 4R tobacco cembranoid as an analgesic agent in both male and female mice that reduces peripheral inflammation in a sex-dependent manner, further supporting the pharmacological targeting of the cholinergic system for pain treatment.

Keywords Inflammatory pain, Tobacco cembranoid, 4R, Hyperalgesia, Paw edema, α7 nicotinic acetylcholine receptors, Persistent analgesia, Macrophage

*Correspondence:
Yarimar Carrasquillo
yarimar.carrasquillo@nih.gov
Full list of author information is available at the end of the article

Background

Nicotiana plants, commonly referred to as tobacco plants, were used by many cultures in the past for a wide range of medicinal purposes, such as wound and burn healing, pain relief, and as a therapeutic option for different diseases [1–3]. Nicotine is the best-known alkaloid of the tobacco plant and is known to bind to all nicotinic cholinergic receptors [4]. Endogenously, nicotinic acetylcholine receptors (nAChRs) can be activated by acetylcholine and have been implicated in various physiological functions such as cognition, inflammation, and pain processing [5, 6]. nAChRs are ligand-gated ion channels found throughout the nervous system and are also found in subsets of immune cells [7–9]. Preclinical studies have shown the therapeutic potential of targeting nAChRs for their anti-inflammatory effects via their modulation of the innate immune response [8].

Consistent with the proposed function of the cholinergic system in pain processing and inflammation, previous studies in rodents have shown that a basal cholinergic tone modulates nociceptive processing. Specifically, the cholinergic tone is increased following injury, and manipulation of this system by endogenous or exogenous ligands can have analgesic and anti-inflammatory effects [10–12]. Given the highly addictive and harmful properties of nicotine, however, efforts have been made to identify pharmacological alternatives to modulate the cholinergic system to treat pain and inflammation [6, 13].

In addition to nicotine, tobacco plants contain many other chemical compounds, including cyclic diterpenoids called cembranoids found in tobacco leaves, flowers, and smoke [14, 15]. The first identified tobacco cembranoids were isolated by Roberts and Rowland in 1962 [16]. Since then, at least 89 other tobacco cembranoids have been described [17]. Whether tobacco cembranoids contributed to the medicinal properties attributed to the tobacco plant in the past, including wound healing and pain relief, has not been established. In the present study, we began to address this question by evaluating the potential analgesic and anti-inflammatory effects of the tobacco cembranoid (1S, 2E, 4R, 6R, 7E, 11E)-cembra-2,7,11-triene-4,6-diol, abbreviated as 4R. 4R was initially extracted and purified from tobacco leaves, has the molecular formula $C_{20}H_{34}O_2$, and the chemical structure is shown in Fig. 1. We selected 4R for this study because it is one of the best functionally characterized tobacco cembranoids [18–22]. Importantly, 4R has been previously shown to have anti-inflammatory and neuroprotective effects and to inhibit prostaglandin synthesis [20, 23–27].

Additional studies have further shown that 4R binds to nAChRs and inhibits three human nAChRs subtypes: neuronal α4β2 (IC50 = 19.1 μM) and α3β4 (IC50 = 2.2 μM) and the embryonic muscle AChR α1β1γδ-AChR (IC50 = 6.6 μM), demonstrating that 4R is a nicotinic receptor ligand [15, 28]. Among the different types of nAChRs, the α7 nAChR has received increasing attention as a potential therapeutic target for chronic inflammation and neuropathic pain [29–31]. Consistent with this, α7 nAChRs have been shown to be expressed in most types of immune cells, including macrophages, T-cells, B-cells, mast cells, and neutrophils [31–34]. Studies have further shown that pharmacological activation of α7 nAChRs reduces inflammation and that deficiencies in α7 nAChRs exacerbate inflammation [32, 35–38]. At the behavioral level, α7 nAChR agonists have been shown to ameliorate pain in various animal pain models [31, 33, 39, 40]. Together these studies strongly position α7 nAChRs as a critical determinant of inflammation and pain-related behaviors.

Based on these combined findings and the proposed function of the cholinergic system in pain modulation and inflammation, we hypothesized that 4R could also decrease injury-induced hypersensitivity in a mouse model of inflammatory pain via modulation of α7 nAChRs. To test these hypotheses, we employed multidisciplinary approaches including pharmacology, behavioral pain assays, genetically modified mice, histology, and flow cytometry. Our pharmacological experiments demonstrate that inflammation-induced peripheral hypersensitivity is reduced with systemic 4R treatment in both male and female mice. Measurements of paw edema and histological assessment of paw samples further show that 4R reduces peripheral inflammation in a sex-dependent manner. Additionally, using Methyllycaconitine (MLA), a selective antagonist of α7 nAChRs, we demonstrate that the anti-hyperalgesic and anti-inflammatory effects of 4R are mediated through α7 nAChRs. Flow cytometry and immunohistochemical analyses of paw samples from *Chrna7*-Cre::Ai9 mice, which are genetically modified to express tdTomato in α7 nAChRs + cells, further indicate that a subset of macrophages and T-cells expresses the α7 nAChRs. However, no measurable changes in the number of α7 nAChR-expressing immune cells were observed following inflammation. Together, our results identified a novel analgesic function for 4R and further support the use of pharmacological agents targeting the cholinergic system to treat pain and inflammation.

Materials and methods

Mice

Male and female C57BL/6 J (Jackson Labs; stock no. 00064) mice were used for all the behavioral experiments. To visualize and detect cells expressing α7 nAChRs in histological and flow cytometric experiments, we used the genetically modified mice described

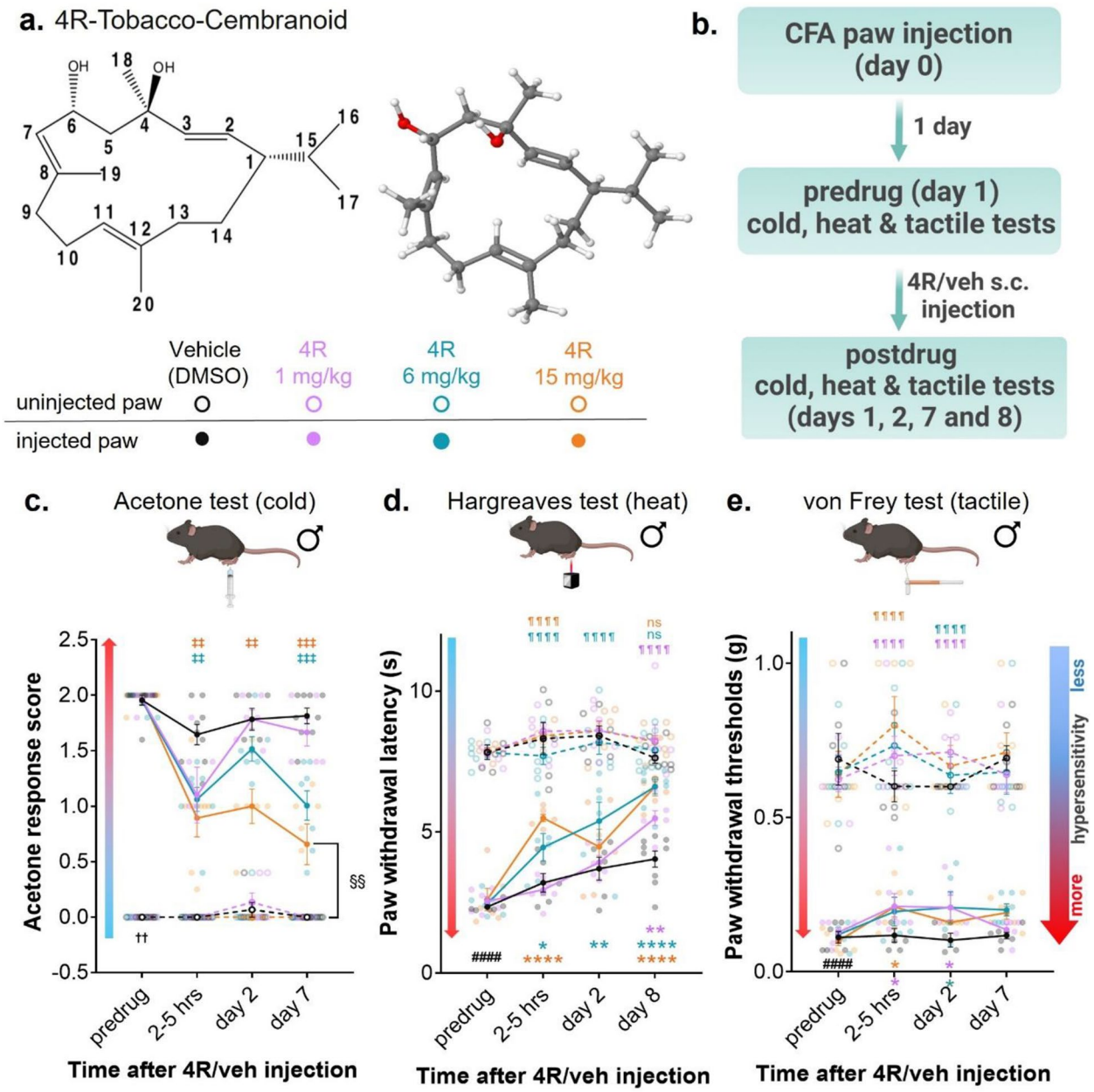

Fig. 1 Systemic administration of 4R tobacco cembranoid reduces inflammation-induced peripheral hypersensitivity (**a**) Chemical structure (left panel) and 3D molecular model (right panel) of 4R-tobacco cembranoid. Oxygen, hydrogen, and carbon atoms are colored red, white, and grey, respectively. (**b**) Experimental timeline for acetone (cold), Hargreaves (heat) and von Frey (tactile) tests in CFA-injected and non-injected hind paws before and at different times after 4R (1, 6 and 15 mg/kg) or vehicle administration. (**c**) Acetone response score, (**d**) withdrawal latency to heat stimulation (**e**) withdrawal threshold to tactile stimulation. All values are expressed as mean ± SEM. $n = 4–9$ animals per treatment and test. Two-way ANOVA followed by posthoc Tukey's multiple comparisons test: CFA-injected paw vs uninjected paw in pre-drug vehicle (veh) conditions, $p < 0.0001$ (####), 4R treated CFA-injected paw vs vehicle uninjected paw, $p < 0.0001$ (¶ ¶ ¶ ¶); not significant = ns. Two-way ANOVA followed by post hoc Dunnett's multiple comparisons test: CFA-injected paws in vehicle vs 4R systemic treatment of the same time-point, $p < 0.05$ (*), $p < 0.01$ (**), $p < 0.001$ (***), $p < 0.0001$ (****). Wilcoxon matched-pairs signed rank test: CFA-injected paw vs uninjected paw in pre-drug vehicle (veh) conditions, $p < 0.01$ (††), Non-parametric Mann–Whitney multiple comparisons test followed by Holm-Šídák method; CFA-injected paws in vehicle vs 4R systemic treatment of the same time-point, adjusted $p < 0.01$ (‡‡), adjusted $p < 0.001$ (‡‡‡); vehicle (veh) uninjected paw (day 7) vs 4R 15 mg/kg CFA-injected paw (day 7), adjusted $p > 0.05$ (§§). Results of multiple comparisons between vehicle (veh) and 4R 1 mg/kg, 6 mg/kg or 15 mg/kg are shown in purple, teal, and orange, respectively

below. *Chrna7*-cre heterozygous male and female mice, stock Tg(Chrna7-cre)NP348Gsat/Mmucd, RRID:MMRRC_034694-UCD, were obtained from the Mutant Mouse Resource and Research Center (MMRRC) at University of California at Davis, an NIH-funded strain repository, and was donated to the MMRRC by Nathaniel Heintz, Ph.D., The Rockefeller University, GENSAT and Charles Gerfen, Ph.D., National Institutes of Health, National Institute of Mental Health. *Chrna7*-cre heterozygous male and female mice were backcrossed to C57BL/6NJ (Jackson Labs; stock no. 005304) for ten generations. *Chrna7*-cre heterozygous male and female mice in C56BL/6NJ background were then crossed with homozygous Ai9 (The Jackson Laboratory, stock no. 007909). The offspring, referred to in this study as $\alpha7^{tdTomato}$, were used for immunohistochemistry (IHC) and flow cytometry experiments. The genotype of offspring mice was assessed for the presence of Cre-recombinase using DNA from tail biopsies and polymerase chain reaction (PCR, Transnetyx). The following primer sequences were used: TTAATCCATATTGGCAGAACGAAA ACG (forward) and CAGGCTAAGTGCCTTCTC TACA (reverse).

Animals were housed in groups of 3–5 littermates in a temperature-controlled facility, with ad libitum access to food and water under reversed 12 h/12 h light/dark cycle (9 pm to 9 am light). All behavioral experiments were performed during the dark phase under red light. For behavior experiments, one week prior to experiments, mice were transferred in pairs to a new home cage divided with perforated plexiglass, with one mouse in each compartment. Mice were handled daily for five days before behavioral testing, as previously described [41]. Procedures performed with mice were approved by the Animal Care and Use Committee of the National Institute of Neurologic Disorders and Stroke, the National Institute of Deafness and Other Communication Disorders, and the University of Texas at Dallas Institutional Animal Care and Use Committee per the National Institutes of Health (NIH) guidelines. All behavioral experiments were performed by an investigator blind to experimental treatments. Pairs of animals within a home cage were randomly assigned to individual experimental groups. After treatment, mice were returned to their original home cage. This randomization system allowed mice with the same treatment to be housed together. Male and female mice were never tested simultaneously in the same behavior room. All experimental procedures were replicated at least two times. For the behavioral experiments, the minimum sample size per sex was determined by a power calculation using G*power (version 3.1.9.2) with effect size (f) set to 0.75, at 95% power with a set to 0.05 [42–44].

CFA model of inflammatory pain and behavioral tests

Mice were lightly anesthetized with isoflurane (0.5%–1% at a flow rate of 0.5 L/min), and 10 µL of Complete Freund's Adjuvant (CFA, F5881, Sigma Aldrich) was injected subcutaneously into the plantar area of the right hind paw using an insulin syringe (Sure Comfort 29 g×1/2″ 3/10 cc). Day 0 is defined as the day of CFA injection. Drug solutions used for systemic injections (vehicle or 4R) were made fresh on the day of administration, and a single subcutaneous (s.c.) injection of 56—70 µL was administered into the loose skin over the shoulder on day 1. CFA-induced inflammation and hyperalgesia were assessed on day 1 before s.c. injection of vehicle or 4R (1, 6, or 15 mg/kg body weight). The doses of 4R were selected based on previous pharmacokinetic studies in rats [45] and extrapolated to mice to account for species differences as previously described [46]. The effects of s.c. treatment with 4R or vehicle on CFA-induced inflammation and hyperalgesia were assessed on days 1, 2, 7, and 8 after the injections. Day 1 effects were measured 2–5 h after s.c. injections.

To evaluate the contribution of α7 nAChRs, we used the α7 nAChRs selective antagonist, Methyllycaconitine (MLA). For these experiments, mice received a single vehicle or MLA (10 mg/kg body weight) injection subcutaneously 15 min before the injection of vehicle or 4R (15 mg/kg body weight). This dose of MLA has been shown to effectively block the anti-nociceptive effects of pharmacological treatments targeting α7 nAChRs [47, 48]. The rest of the experiments were performed identically to the 4R experiments described above.

The dorsal–ventral diameter of the CFA-treated and untreated hind paws were measured as an indirect measurement of inflammation using a microcaliper (UX-97152–17, Cole Palmer). For all behavioral tests, animals were individually placed inside a custom-made white plexiglass testing chamber (11×11x13 cm) on an elevated mesh (for acetone and von Frey tests) (NIH Section on Instrumentation) or a glass platform heated to 30°C (for the heat test).

von Frey

Withdrawal thresholds to tactile stimulation, defined as paw withdrawal followed by a brief shake or lick of the paw, were measured using graded monofilaments (North Coast Medical, Inc. San Jose, CA) after animals were habituated to the testing chamber and room for 3 h, as previously described [49]. Starting with the smallest filament, the tip was pressed against the plantar area of the hind paw until it bent at 30° for approximately one

second. The procedure was repeated five times per filament. The filament that elicited paw withdrawal at least three out of five times was recorded as the mechanical threshold for that trial. The average of three trials was considered the mechanical threshold of the paw tested.

Acetone test

Cold sensitivity was assessed using the acetone evaporative test [50], adapted to test mice. An acetone drop was briefly applied to the plantar region of the hind paw and nocifensive responses were scored using a modified scoring system previously described [49, 51]. The scoring system ranges from 0 to 2, indicating the following: 0 = no reaction or an immediate transient lifting or shaking of the hind paw that subsides immediately, 1 = lifting, licking, and/or shaking of the hind paw, which continues beyond the initial application, but subsides within 5 s, and 2 = protracted, repeated lifting, licking, and/or shaking of the hind paw. The response to acetone application was observed for approximately one minute and scored. The average of three stimulations per hind paw represents the score of the paw tested.

Hargreaves test

The Hargreaves test was used to assess sensitivity to heat, as previously reported [49]. Animals were habituated for one hour in ventilated testing chambers placed on a heated glass surface (30°C). Paw withdrawal latencies were measured after stimulating the hind paw with a heat light aimed at the center of the plantar surface using an active intensity of 25 (intensity of light source defined by the manufacturer; IITC Life Science, Woodland Hills, CA). Three to five stimulations per hind paw were logged, and the average was reported.

Drugs

The tobacco cembranoid (1S,2E,4R,6R,7E,11E)-2,7,11-cembratriene-4,6-diol (4R) was obtained from El Sayed Research Foundation; University of Louisiana–Monroe, College of Pharmacy and prepared as previously described [52]. The purity of the batch used for these experiments was more than 98%, determined by Nuclear Magnetic Resonance (NMR) spectroscopy and thin layer chromatography (TLC). 4R was dissolved in dimethyl sulfoxide (DMSO) (D2650; Sigma Aldrich) to make a stock solution with a final concentration of 20 mM. The selective antagonist MLA (1029; Tocris) was dissolved in saline to make a 10 mM stock solution. A 2.5 mM 4R solution was made from the 4R (20 mM) stock solution to produce the lowest 4R dose injected (1 mg/kg body weight). In all experiments, mice were tested in cohorts of 6 and always included at least one animal per dose. Individual doses per animal were calculated based on body weight. All syringes in a cohort were brought to the same final volume with DMSO as part of the blinding process for testing. The range of injected volumes used was 56 – 70 µL.

Samples origin for histology

Mice were injected with CFA on the right hind paw seven days before collecting the samples. 24 h after CFA injection, mice were treated with 4R (15 mg/kg) or vehicle (DMSO) by a single s.c. injection. On day eight after the CFA injection, mice were anesthetized with 1.25% Avertin (2,2,2-tribromoethanol and tert-amyl alcohol in 0.9% NaCl; 0.025 ml/g body weight) followed by transcardial perfusion with 37 °C 0.9% NaCl to clear the blood and 100 ml of ice-cold 4% paraformaldehyde (Sigma, 158127) made in 1 × phosphate-buffered saline (PBS) (pH = 7.4 ± 0.05) (4% PFA/PB). After transcardial perfusion, the left (uninjected) and right (injected) hind paws were removed by cutting the tibia and fibula halfway between the knee and ankle joints. Collected samples were post-fixed with 4% PFA/PB overnight at 4°C and sent to Histoserv Inc. (Germantown, MD) the next day for histological processing. After mild decalcification for 3.5 weeks, hind paws were embedded in paraffin blocks and a total of three 10-µm cross-sectional cuts of the foot pad were collected per hind paw at the site of intraplantar injection and fixed to glass slides for subsequent staining. Two of these sections were collected 20 µm apart and the third one was collected 100 µm apart.

H&E staining and Iba1 immunofluorescence

One of the collected cross-sectioned cuts of the hind paws foot pad was stained with hematoxylin and eosin (H&E) by Histoserv (Germantown, MD). The other two sections, separated by 100 µm, were used for immunostaining Histoserv (Germantown, MD). Slides were air-dried, fixed for 2 min in neutral buffered formalin with methanol, and air-dried again. 5% normal goat serum (NGS) with 0.5% bovine serum albumin (BSA) and 0.1% Triton X-100 was used for blocking solution. Sections were incubated overnight at 4 °C in rabbit anti-ionized calcium-binding adaptor molecule 1 (Iba1) (1:2000; 019–19741; Fujifilm Wako Pure Chemical Corporation) diluted in 1.5% NGS, 0.5% BSA, and 0.1% Triton X-100. Sections then were incubated in secondary antibody tagged with fluorophore Alexa Fluor 647-conjugated goat anti-rabbit (1:100, Invitrogen, A21244). Finally, slides were wet mounted using Prolong Gold with DAPI (P36931, Invitrogen) and a coverslip, air dried, and the edges were sealed.

Tissue collection and cell isolation for flow cytometry

On day 8, mice were deeply anesthetized using isoflurane and euthanized via decapitation. Ipsi- and contralateral hind paws were collected for flow cytometry. The whole foot was removed at the ankle joint, and plantar skin (including the subdermal layer) from the foot pad was dissected into ice-cold sterile 1 × DPBS (Hyclone, SH30028) before downstream processing. Fresh skin samples were centrifuged at 400 × g for 3 min, and supernatants were removed and treated with a mix of Collagenase A (Sigma, 10103586001) and Collagenase D (Sigma, 1188866001) with 10% v/v of papain (Roche, 10108014001) in HBSS (Gibco, 14170–112) for 90 min, with vortexing every 30 min. Cells were centrifuged at 400 × g, and the pellet was resuspended in Enzyme T (Sigma, 10109886001) (soybean trypsin inhibitor made in 1:1 bovine serum albumin and DMEM/F12 media (Thermo-Fisher, 10565161) supplemented with 10% fetal bovine serum (FBS) (Hyclone, SH30088.03) and 1% pen/strep (Sigma, P4333)) to stop the enzymatic reaction. Digested tissues were triturated using a 1 mL pipette tip and passed through a 70-µm nylon mesh cell strainer (Sigma, CLS431751-50EA), with a subsequent wash using flow buffer (0.5% bovine serum albumin with 0.02% glucose (Sigma, G7528) made in 1 × DPBS). The resultant suspension was further processed for flow cytometry (see details below).

Flow cytometry

Freshly dissociated paw skin cells from plantar skin were suspended in ice-cold sterile 1 × DPBS and centrifuged at 400 × g for 3 min. The cells were resuspended in flow buffer (0.5% bovine serum albumin with 0.02% glucose (Sigma, G7528) made in 1 × DPBS), with blocking antibody (anti-CD16/32 purified (1:2000) (eBioscience, 16016185)) for 20 min to block Fc receptors. Samples were then incubated with pre-conjugated extracellular flow antibodies, F4/80 (BioLegend 123141) and CD3 (eBioscience, 56003282) for 45 min. Samples were washed with flow buffer, centrifuged at 400 × g for 3 min, and resuspended in a DAPI wash for 5 min. Samples were centrifuged at 400 × g for 3 min, washed twice using flow buffer, and resuspended in flow buffer. Appropriate compensation controls and isotypes were used for determination and gating. After gating DAPI-positive cells (to determine debris), $\alpha7^{tdT}$ ($tdTomato^{+}$ cre driven nAChRs) cells were gated to determine the overlap with F4/80 and CD3. Stained samples were analyzed using a Special Order (4-laser) Becton–Dickinson Fortessa analyzer (Red Oaks, CA), and data were analyzed using FlowJo and FCS Express software (De NoVo Software, Los Angeles, CA). Experimenters were blinded to sex and treatments.

Data analysis and statistics

Data are expressed as mean ± standard error of the mean (S.E.M.). Statistical analyses were performed using Prism (v. 9, GraphPad Software Inc., La Jolla, CA, U.S.A.). Normality was assessed in all data sets using the Kolmogorov–Smirnov test. For normally distributed data, paired t-test was used to compare the means of two dependent groups with one variable, two-way analysis of variance (ANOVA) test was used to compare the means of two or more independent groups with two independent variables, and repeated measures two-way ANOVA was used for complete data sets to compare two or more dependent groups with two independent variables. Šidák's, Tukey's, or Dunnett's posthoc multiple comparison tests were used for independent comparisons of selected data, for comparing between groups, and to compare experimental groups to a single control group, respectively. For non-normally distributed data with four independent groups and one variable, we used the Kruskal–Wallis test followed by Dunn's posthoc multiple comparison test for independent comparison of selected data. For categorical type of data, we employed non-parametric Wilcoxon matched-pairs signed rank test to compare two dependent groups with one variable, non-parametric Mann–Whitney multiple comparisons test, corrected with the Holm-Šídák method, to compare two independent groups with two independent variables, and the non-parametric Kruskal–Wallis test followed by Dunn's posthoc multiple comparisons test to compare four dependent groups with one variable. *P*-values < 0.05 were recognized as significant. See Table 1 for a detailed description of statistics.

Results

Systemic administration of 4R tobacco cembranoid reduces inflammation-induced peripheral hypersensitivity in male mice

The CFA mouse model of persistent inflammatory pain was used to test the hypothesis that systemic administration of 4R tobacco cembranoid decreases inflammation-induced peripheral hypersensitivity. CFA injection in the paw has been shown to cause swelling and hypersensitivity to cold, heat, and tactile stimuli [53, 54]. The potential antinociceptive effects of systemic administration of 4R on cold, heat, and tactile sensitivity in the CFA-injected and uninjected hind paws were measured at different time points (pre-drug, and 2–5 h, day 2, day 8 after 4R or vehicle administration) using acetone, Hargreaves, and von Frey test, respectively (Fig. 1a-e). Three doses of 4R (1, 6, and 15 mg/kg by body weight) or vehicle, injected subcutaneously one day after the CFA injection, were evaluated (Fig. 1b).

Table 1 Statistical analyses

Figure	Type of Data	Type of Test	Sample Size	Statistical Data
Figure 1				
1c (Acetone; injected vs non-injected paw)	Categorical	Non-parametric Wilcoxon matched-pairs signed rank test	vehicle predrug = 9 mice	Wilcoxon matched-pairs signed rank test: DMSO non-injected paw vs. DMSO injected paw pre-drug, $p = 0039$
1c (Acetone; injected paw max. effect vs uninjected paw)	Categorical	Non-parametric Mann–Whitney multiple comparisons test, Holm-Šídák method	vehicle uninjected paw day 7 = 9 mice; 4R 15 mg/kg day 7 = 7 mice	Mann–Whitney test, DMSO non-injected paw day 7 vs. 4R 15 mg/kg day 7 injected paw, adjusted $p = 0.0086$
1d (Hargreaves; injected vs non-injected paw)	Normal	Two-way ANOVA followed by Tukey's multiple comparisons test	vehicle (predrug, 2–5 h., day 2) = 6 mice; vehicle day 8 = 9 mice; 4R 1 mg/kg (all time points) = 6 mice; 4R 6 mg/kg (predrug, 2–5 h., day 2) = 6 mice; 4R 6 mg/kg day 8 = 8 mice; 4R 15 mg/kg (predrug, 2–5 h., day 2) = 6 mice; 4R 15 mg/kg day 8 = 7 mice	Two-way ANOVA time: $F (3, 172) = 37.71$; $p < 0.0001$ treatment: $F (7, 172) = 173.3$; $p < 0.0001$ interaction: $F (21, 172) = 6.204$; $p < 0.0001$ *posthoc*: Tukey's multiple comparisons test CFA-injected paw vs uninjected paw in veh conditions: $p < 0.0001$ (predrug); $p < 0.0001$ (2–5 h, 6 mg/kg and 15 mg/kg); $p < 0.0001$ (day 2, 6 mg/kg); $p < 0.0001$ (day 8, 1 mg/kg); $p = 0.2131$ (day 8, 6 mg/kg); $p = 0.2354$ (day 8, 15 mg/kg)
1d (Hargreaves; injected paw time course)	Normal	Two-way ANOVA followed by Dunnett's multiple comparisons test	vehicle (predrug, 2–5 h., day 2) = 6 mice; vehicle day 8 = 9 mice; 4R 1 mg/kg (all time points) = 6 mice; 4R 6 mg/kg (predrug, 2–5 h., day 2) = 6 mice; 4R 6 mg/kg day 8 = 8 mice; 4R 15 mg/kg (predrug, 2–5 h., day 2) = 6 mice; 4R 15 mg/kg day 8 = 7 mice	Two-way ANOVA time: $F (3, 86) = 59.20$; $p < 0.0001$ treatment: $F (3, 86) = 17.87$; $p < 0.0001$ interaction: $F (9, 86) = 3.671$; $p = 0.0006$ *posthoc*: Dunnett's multiple comparisons test 2–5 h: $p = 0.0395$ for DMSO vs. 4R 6 mg/kg; $p < 0.0001$ for DMSO vs. 4R 15 mg/kg day 2: $p = 0.0035$ for DMSO vs. 4R 6 mg/kg day 8: $p = 0.0067$ for DMSO vs. 4R 1 mg/kg; $p < 0.0001$ for DMSO vs. 4R 6 mg/kg and DMSO vs. 4R 15 mg/kg
1d (Hargreaves; non-injected paw time course)	Normal	Two-way ANOVA	vehicle (predrug, 2–5 h., day 2) = 6 mice; vehicle day 8 = 9 mice; 4R 1 mg/kg (all time points) = 6 mice; 4R 6 mg/kg (predrug, 2–5 h., day 2) = 6 mice; 4R 6 mg/kg day 8 = 8 mice; 4R 15 mg/kg (predrug, 2–5 h., day 2) = 6 mice; 4R 15 mg/kg day 8 = 7 mice	Two-way ANOVA time: $F (3, 86) = 2.964$; $p = 0.0366$ treatment: $F (3, 86) = 1.450$; $p = 0.2338$ interaction: $F (9, 86) = 0.4422$; $p = 0.9083$

Table 1 (continued)

Figure	Type of Data	Type of Test	Sample Size	Statistical Data
1e (von Frey; injected vs non-injected paw)	Normal	Two-way ANOVA followed by Tukey's multiple comparisons test	vehicle (predrug, 2–5 h.) = 6 mice; vehicle day 2 = 4 mice; vehicle day 8 = 7 mice; 4R 1 mg/kg (predrug, 2–5 h) = 6 mice; 4R 1 mg/kg (day 2, day 8) = 5 mice; 4R 6 mg/kg (predrug, 2–5 h., day 8) = 6 mice; 4R 6 mg/kg day 2 = 5 mice; 4R 15 mg/kg (predrug, 2–5 h., day 8) = 6 mice; 4R 15 mg/kg day 2 = 4 mice	Two-way ANOVA time: F (3, 148) = 2.378; $p = 0.0722$ drug treatments: F (7, 148) = 121.8; $p < 0.0001$ interaction: F (21, 148) = 0.7112; $p = 0.8167$ *posthoc*: Tukey's multiple comparisons test CFA-injected paw vs uninjected paw in veh conditions; $p < 0.0001$ (predrug); $p < 0.0001$ (2–5 h, 1 mg/kg and 15 mg/kg); $p < 0.0001$ (day 2, 1 mg/kg, 6 mg/kg)
1e (von Frey; injected paw time course)	Normal	Two-way ANOVA followed by Dunnett's multiple comparisons test	vehicle (predrug, 2–5 h.) = 6 mice; vehicle day 2 = 4 mice; vehicle day 8 = 7 mice; 4R 1 mg/kg (predrug, 2–5 h) = 6 mice; 4R 1 mg/kg (day 2, day 8) = 5 mice; 4R 6 mg/kg (predrug, 2–5 h., day 8) = 6 mice; 4R 6 mg/kg day 2 = 5 mice; 4R 15 mg/kg (predrug, 2–5 h., day 8) = 6 mice; 4R 15 mg/kg day 2 = 4 mice	Two-way ANOVA time: F (3, 74) = 4.861; $p = 0.0038$ drug treatments: F (3, 74) = 4.891; $p = 0.0037$ interaction: F (9, 74) = 1.062; $p = 0.4008$ *posthoc*: Dunnett's multiple comparisons test 2–5 h: $p = 0.0403$ for DMSO vs. 4R 1 mg/kg; $p = 0.0476$ for DMSO vs. 4R 15 mg/kg day 2: $p = 0.0487$ for DMSO vs. 4R 1 mg/kg; $p = 0.0479$ for DMSO vs. 4R 6 mg/kg day 8: $p = 0.0067$ for DMSO vs. 4R 1 mg/kg; $p < 0.0001$ for DMSO vs. 4R 6 mg/kg and DMSO vs. 4R 15 mg/kg
1e (von Frey; non-injected paw time course)	Normal	Two-way ANOVA	vehicle (predrug, 2–5 h.) = 6 mice; vehicle day 2 = 4 mice; vehicle day 8 = 7 mice; 4R 1 mg/kg (predrug, 2–5 h) = 6 mice; 4R 1 mg/kg (day 2, day 8) = 5 mice; 4R 6 mg/kg (predrug, 2–5 h., day 8) = 6 mice; 4R 6 mg/kg day 2 = 5 mice; 4R 15 mg/kg (predrug, 2–5 h., day 8) = 6 mice; 4R 15 mg/kg day 2 = 4 mice	Two-way ANOVA time: F (3, 74) = 0.7107; $p = 0.5487$ treatment: F (3, 74) = 0.5522; $p = 0.6483$ interaction: F (9, 74) = 0.7197; $p = 0.6892$
Figure 2				
2b (Acetone; injected vs. non-injected paw; day 2)	Categorical	Non-parametric Mann–Whitney multiple comparisons test, Holm-Šídák method	vehicle and 4R 15 mg/kg = 6 mice	Mann–Whitney multiple comparisons test, Holm-Šídák method; DMSO injected paw vs. DMSO uninjected paw: adjusted $p = 0.0043$; DMSO uninjected vs 4R 15 mg/kg in injected paw: adjusted $p = 0.0152$
2b (Acetone; veh vs. 4R; day 2)	Categorical	Non-parametric Mann–Whitney multiple comparisons test, Holm-Šídák method	vehicle and 4R 15 mg/kg = 6 mice	Mann–Whitney multiple comparisons test, Holm-Šídák method; DMSO vs. 4R 15 mg/kg in injected paw: adjusted $p = 0.0258$

Table 1 (continued)

Figure	Type of Data	Type of Test	Sample Size	Statistical Data
2c (Hargreaves; injected vs non-injected paw; day 2)	Normal	Two-way ANOVA followed by Šídák's multiple comparisons test	vehicle and 4R 15 mg/kg = 6 mice	Two-way ANOVA paw side: F (1, 20) = 384.3; $p < 0.0001$ treatment: F (1, 20) = 38.57; $p < 0.0001$ interaction:F (1, 20) = 26.88; $p < 0.0001$ *posthoc*: Šídák's multiple comparisons test adjusted $p < 0.0001$ for CFA-injected paw vs uninjected paw in veh conditions;
2c (Hargreaves; 4R injected vs. DMSO non-injected paw; day 2)	Normal	Two-way ANOVA followed by Tukey's multiple comparisons test	vehicle and 4R 15 mg/kg = 6 mice	Two-way ANOVA paw side: F (1, 20) = 384.3; $p < 0.0001$ treatment: F (1, 20) = 38.57; $p < 0.0001$ interaction:F (1, 20) = 26.88; $p < 0.0001$ *posthoc*: Tukeys multiple comparisons test adjusted $p < 0.0001$ for 4R 15 mg/kg CFA-injected paw vs uninjected paw in veh conditions
2c (Hargreaves;veh vs 4R; day 2)	Normal	Two-way ANOVA followed by Šídák's multiple comparisons test	vehicle and 4R 15 mg/kg = 6 mice	Two-way ANOVA paw side: F (1, 20) = 384.3; $p < 0.0001$ treatment: F (1, 20) = 38.57; $p < 0.0001$ interaction: F (1, 20) = 26.88; $p < 0.0001$ *posthoc*: Šídák's multiple comparisons test $p < 0.0001$ for DMSO vs. 4R 15 mg/kg in injected paw $p = 0.7260$ for DMSO vs. 4R 15 mg/kg in non-injected paw
2d (von Frey; injected vs non-injected paw; day 2)	Normal	Two-way ANOVA followed by Šídák's multiple comparisons test	vehicle and 4R 15 mg/kg = 6 mice	Two-way ANOVA paw side: F (1, 20) = 277.2, $p < 0.0001$ treatment: F (1, 20) = 1.213; $p = 0.2838$ interaction:F (1, 20) = 1.213; $p = 0.2838$ *posthoc*: Šídák's multiple comparisons test $p < 0.0001$ for CFA-injected paw vs uninjected paw in veh conditions

Table 1 (continued)

Figure	Type of Data	Type of Test	Sample Size	Statistical Data
2d (von Frey; veh vs 4R; day 2)	Normal	Two-way ANOVA followed by Šídák's multiple comparisons test	vehicle and 4R 15 mg/kg = 6 mice	Two-way ANOVA paw side:F (1, 20) = 277.2; $p < 0.0001$ treatment: F (1, 20) = 1.213; $p = 0.2838$ interaction: F (1, 20) = 1.213; $p = 0.2838$ *posthoc*: Šídák's multiple comparisons test $p = 0.2518$ for DMSO vs. 4R 15 mg/kg in injected paw $p > 0.9999$ for DMSO vs. 4R 15 mg/kg in non-injected paw
2e (Acetone; injected vs non-injected paw; day 7)	Categorical	Non-parametric Mann–Whitney multiple comparisons test, Holm-Šídák method	vehicle and 4R 15 mg/kg = 6 mice	Mann–Whitney multiple comparisons test, Holm-Šídák method; DMSO injected paw vs. DMSO uninjected paw: adjusted $p = 0.0043$, DMSO uninjected vs 4R 15 mg/kg in injected paw: adjusted $p = 0.0043$
2f (Hargreaves; injected vs non-injected paw; day 7)	Normal	Two-way ANOVA followed by Šídák's multiple comparisons test	vehicle and 4R 15 mg/kg = 6 mice	Two-way ANOVA paw side: F (1, 20) = 42.74; $p < 0.0001$ treatment: F (1, 20) = 7.807; $p = 0.0112$ interaction:F (1, 20) = 5.150; $p = 0.0345$ *posthoc*: Šídák's multiple comparisons test adjusted $p < 0.0001$ for CFA-injected paw vs uninjected paw in veh conditions,
2f (Hargreaves; 4R injected vs. DMSO non-injected paw; day 7)	Normal	Two-way ANOVA followed by Tukey's multiple comparisons test	vehicle and 4R 15 mg/kg = 6 mice	Two-way ANOVA paw side: F (1, 20) = 42.72; $p < 0.0001$ treatment: F (1, 20) = 7.807; $p = 0.0112$ interaction:F (1, 20) = 5.150; $p = 0.0345$ *posthoc*: Tukeys multiple comparisons test adjusted $p = 0.0679$ for 4R 15 mg/kg CFA-injected paw vs uninjected paw in veh conditions

Table 1 (continued)

Figure	Type of Data	Type of Test	Sample Size	Statistical Data
2f (Hargreaves;veh vs 4R; day 7)	Normal	Two-way ANOVA followed by Šídák's multiple comparisons test	vehicle and 4R 15 mg/kg = 6 mice	Two-way ANOVA paw side: F (1, 20) = 42.74; $p < 0.0001$ treatment: F (1, 20) = 7.807; $p = 0.0112$ interaction: F (1, 20) = 5.150; $p = 0.0345$ *posthoc*: Šídák's multiple comparisons test $p = 0.0037$ for DMSO vs. 4R 15 mg/kg in injected paw $p = 0.9185$ for DMSO vs. 4R 15 mg/kg in non-injected paw
2 g (von Frey; injected vs non-injected paw; day 7)	Normal	Two-way ANOVA followed by Šídák's multiple comparisons test	vehicle and 4R 15 mg/kg = 6 mice	Two-way ANOVA paw side: F (1, 20) = 74.43; $p < 0.0001$ treatment: F (1, 20) = 0.8013; $p = 0.3814$ interaction: F (1, 20) = 0.01463; $p = 0.9049$ *posthoc*: Šídák's multiple comparisons test $p < 0.0001$ for CFA-injected paw vs uninjected paw in veh conditions
2g (von Frey; veh vs 4R; day 7)	Normal	Two-way ANOVA followed by Šídák's multiple comparisons test	vehicle and 4R 15 mg/kg = 6 mice	Two-way ANOVA paw side: F (1, 20) = 74.43; $p < 0.0001$ treatment: F (1, 20) = 0.8013; $p = 0.3814$ interaction: F (1, 20) = 0.01463; $p = 0.9049$ *posthoc*: Šídák's multiple comparisons test $p = 0.7304$ for DMSO vs. 4R 15 mg/kg in injected paw $p = 0.8320$ for DMSO vs. 4R 15 mg/kg in non-injected paw

Table 1 (continued)

Figure	Type of Data	Type of Test	Sample Size	Statistical Data
Figure 3				
3b (thickness of injected vs non-injected paw, male)	Normal	Two-way ANOVA followed by Tukey's multiple comparisons test	vehicle (predrug, 2–5 h., day 2) = 16 mice; vehicle (day 3, day 7) = 12 mice; vehicle day 8 = 9; 4R 1 mg/kg (predrug, 2–5 h., day 2) = 14 mice; 4R 1 mg/kg (day 3, day 7) = 12 mice; 4R 1 mg/kg day 8 = 6 mice; 4R 6 mg/kg (predrug, 2–5 h., day 2) = 16 mice; 4R 6 mg/kg (day 3, day 7) = 12 mice; 4R 6 mg/kg day 8 = 8 mice; 4R 15 mg/kg (predrug, 2–5 h., day 2) = 14 mice; 4R 15 mg/kg (day 3, day 7) = 12 mice; 4R 15 mg/kg day 8 = 7 mice	Two-way ANOVA time: F (5, 564) = 45.20; $p < 0.0001$ drug treatments: F (7, 564) = 447.0; $p < 0.0001$ interaction: F (35, 564) = 8.479; $p < 0.0001$ *posthoc*: Tukey's multiple comparisons test CFA-injected paw vs uninjected paw in veh conditions; $p < 0.0001$ (predrug); $p < 0.0001$ (day 7, 4R 6 mg/kg)
3b (injected paw thickness time course, male)	Normal	Two-way ANOVA followed by Dunnett's multiple comparisons test	vehicle (predrug, 2–5 h., day 2) = 16 mice; vehicle (day 3, day 7) = 12 mice; vehicle day 8 = 9; 4R 1 mg/kg (predrug, 2–5 h., day 2) = 14 mice; 4R 1 mg/kg (day 3, day 7) = 12 mice; 4R 1 mg/kg day 8 = 6 mice; 4R 6 mg/kg (predrug, 2–5 h., day 2) = 16 mice; 4R 6 mg/kg (day 3, day 7) = 12 mice; 4R 6 mg/kg day 8 = 8 mice; 4R 15 mg/kg (predrug, 2–5 h., day 2) = 14 mice; 4R 15 mg/kg (day 3, day 7) = 12 mice; 4R 15 mg/kg day 8 = 7 mice	Two-way ANOVA time: F (5, 282) = 50.75; $p < 0.0001$ drug treatments: F (3, 282) = 12.64; $p < 0.0001$ interaction:F (15, 282) = 1.301; $p = 0.2007$ *posthoc*: Dunnett's multiple comparisons test day 2: $p = 0.0212$ for DMSO vs. 4R 15 mg/kg day 3: $p = 0.0061$ for DMSO vs. 4R 6 mg/kg; $p = 0.0165$ for DMSO vs. 4R 15 mg/kg day 7: $p = 0.0006$ for DMSO vs. 4R 6 mg/kg; $p = 0.0061$ for DMSO vs. 4R 15 mg/kg day 8: $p = 0.0172$ for DMSO vs. 4R 6 mg/kg; $p = 0.0152$ for DMSO vs. 4R 15 mg/kg
3c (thickness of injected vs non-injected paw, female)	Normal	Two-way RM ANOVA followed by Tukey's multiple comparisons test	vehicle and 4R 15 mg/kg = 6 mice	Two-way RM ANOVA time: F (1.448, 28.95) = 88.41; $p < 0.0001$ drug treatments: F (3, 20) = 520.4; $p < 0.0001$ time X drug treatments: F (15, 100) = 33.57; $p < 0.0001$ *posthoc*: Tukey's multiple comparisons test pre-drug: $p < 0.0001$ for CFA-injected paw vs uninjected paw in veh conditions time: F (5, 60) = 70.27; $p < 0.0001$ drug treatments: F (1, 60) = 0.5000; $p = 0.4822$ interaction: F (5, 60) = 2.675; $p = 0.0301$

Table 1 (continued)

Figure	Type of Data	Type of Test	Sample Size	Statistical Data
3f (injected paw glabrous skin thickness)	Normal	Two-way ANOVA followed by Šídák's multiple comparisons test	Vehicle—male = 6 mice Vehicle—female = 6 mice 4R—male = 5 mice 4R—female = 6 mice	Two-way ANOVA drug treatment: F (1, 19) = 4.647; $p = 0.0441$ sex: F (1, 19) = 0.294; $p = 0.5936$ interaction: F (1, 19) = 0.056; $p = 0.8140$ *posthoc*: Šídák's multiple comparisons test $p = 0.3617$ for Males Vehicle vs. Males 4R $p = 0.1881$ for Females Vehicle vs. Females 4R
3g (injected paw subdermal cell count)	Normal	Two-way ANOVA followed by Šídák's multiple comparisons test	Vehicle—male = 6 mice Vehicle—female = 6 mice 4R—male = 5 mice 4R—female = 6 mice	Two-way ANOVA drug treatment: F (1, 19) = 7.495; $p = 0.0131$ sex: F (1, 19) = 0.4968; $p = 0.48985$ interaction: F (1, 19) = 7.073; $p = 0.0155$ *posthoc:* Šídák's multiple comparisons test $p = 0.0028$ for Males Vehicle vs. Male 4R $p = 0.9980$ for Females Vehicle vs. Females 4R $p = 0.0489$ for Males Vehicle vs. Females Vehicle $p = 0.3484$ for Males 4R vs. Females 4R
Figure 4				
4b (Acetone)	Categorical	Non-parametric Kruskal–Wallis test followed by Dunn's multiple comparisons test	MLA + DMSO, MLA + 4R, Saline + 4R and Saline + DMSO = 6 mice	Kruskal–Wallis test: $p = 0.0076$; posthoc: Dunn's mutiple comparisons test: Saline + 4R vs. MLA + 4R $p = 0.0041$; Saline + DMSO vs. MLA + DMSO $p = 0.7503$;
4c (Hargreaves)	Non-normal	Non-parametric Kruskal–Wallis test followed by Dunn's multiple comparisons test	MLA + DMSO, MLA + 4R, Saline + 4R and Saline + DMSO = 6 mice	Kruskal–Wallis test: $p = 0.0005$; posthoc: Dunn's mutiple comparisons test: Saline + 4R vs. MLA + 4R $p = 0.0058$; Saline + DMSO vs. MLA + DMSO $p = 0.0825$;
4d (thickness of injected vs non-injected paw, male)	Normal	Two-way RM ANOVA followed by Tukey's multiple comparisons test	MLA + DMSO = 6 mice, MLA + 4R = 6 mice, Saline + 4R = 6 mice and Saline + DMSO = 3–6 mice	Two-way ANOVA time: F (1.561, 57.76) = 37.40; $p < 0.0001$ drug treatments: F (7, 37) = 290.5; $p < 0.0001$ interaction: F (35, 185) = 7.757; $p < 0.0001$ *posthoc*: Tukey's multiple comparisons test pre-drug: $p < 0.0001$ for CFA-injected paw vs uninjected paw in veh conditions

Table 1 (continued)

Figure	Type of Data	Type of Test	Sample Size	Statistical Data
4d (injected paw thickness time course, male)	Normal	Two-way RM ANOVA followed by Tukey's multiple comparisons test	MLA + DMSO = 6 mice, MLA + 4R = 6 mice, Saline + 4R = 6 mice and Saline + DMSO = 3–6 mice	Two-way ANOVA time: F (1.403, 28.06) = 52.55; $p < 0.0001$ drug treatments: F (3, 20) = 2.550; $p = 0.0846$ interaction: F (15, 100) = 1.651; $p = 0.0737$ *posthoc*: Tukey's multiple comparisons test day 2: $p = 0.0076$ for Saline + 4R vs. Saline + DMSO day 3: $p = 0.0026$ for Saline + 4R vs. Saline + DMSO day 7: $p = 0.0200$ for Saline + 4R vs. Saline + DMSO; $p = 0.0069$ for MLA + 4R vs. Saline + 4R day 8: $p = 0.0116$ for Saline + 4R vs. Saline + DMSO; $p = 0.0043$ for MLA + 4R vs. Saline + 4R
Figure 5				
5c (injected paw subdermal $\alpha7^{tdT}$ cell count)	Normal	Two-way ANOVA	Vehicle—male = 5 mice Vehicle—female = 4 mice 4R—male = 4 mice 4R—female = 4 mice	Two-way ANOVA drug treatments: F(1, 13) = 0.001727; $p = 0.9675$ sex: F(1, 13) = 0.008159; $p = 0.9294$ interaction: F(1, 13) = 0.6627; $p = 0.4303$
5d (injected paw subdermal Iba-1^+ cell count	Normal	Two-way ANOVA	Vehicle—male = 4 mice Vehicle—female = 4 mice 4R—male = 4 mice 4R—female = 4 mice	Two-way ANOVA drug treatments: F(1, 12) = 0.2515; $p = 0.6251$ sex: F(1, 12) = 0.02600; $p = 0.6251$ interaction: F(1, 12) = 0.8920; $p = 0.3636$
5e (injected paw subdermal colocalized cell count	Normal	Two-way ANOVA	Vehicle—male = 5 mice Vehicle—female = 4 mice 4R—male = 4 mice 4R—female = 4 mice	Two-way ANOVA drug treatments: F(1, 13) = 0.6376; $p = 0.4389$ sex: F(1, 12) = 0.05774; $p = 0.8138$ interaction: F(1, 12) = 0.5835; $p = 0.4586$

Table 1 (continued)

Figure	Type of Data	Type of Test	Sample Size	Statistical Data
5h (injected paw subdermal $\alpha7^{tdT}$ cell count	Normal	Paired t-test	CFA-injected—male = 4 mice	Paired t-test (F4/80)
			uninjected—male = 4 mice	*p* value: 0.5122
			CFA-injected—female = 4 mice	t, df: t = 0.6904, df = 7
			uninjected—female = 4 mice	Paired t-test (CD3 +)
				p value: 0.9088
				t, df: t = 0.1188, df = 7

Detailed information about data structure, statistical tests, sample sizes and statistical results

$F_{(DFn, DFd)}$ Degree of freedom for the numerator of the F ratio, for the denominator of the F ratio, *df* Degrees of freedom

Consistent with previous reports [53, 55], subcutaneous injection of CFA into the hind paw induced hypersensitivity to cold, heat, and tactile stimuli in the injected paw, compared to the uninjected hind paw (Fig. 1c-e). Thus, prior to 4R treatment (pre-drug condition), the response score to acetone paw stimulation was significantly ($p < 0.001$) higher (Fig. 1c), and the withdrawal latencies to heat stimulation were significantly ($p < 0.0001$) shorter (Fig. 1d) in CFA-treated hind paws, compared to the untreated hind paws. Similarly, paw withdrawal thresholds in response to tactile stimulation were significantly ($p < 0.0001$) lower in the CFA-injected paw compared to the uninjected hind paw (Fig. 1e). As expected, CFA-induced persistent hypersensitivity to cold, heat, and tactile stimulation was observed in the injected hind paws of control mice (systemically treated with vehicle) for 8 days after CFA injection.

As illustrated in Fig. 1c-e, a single injection of 4R reduces CFA-induced hypersensitivity in a dose and time-dependent manner. Following the administration of the lowest dose of 4R (1 mg/kg), for example, a significant ($p < 0.01$) decrease in response scores to acetone stimulation was observed in the CFA-injected paw 2–5 h after 4R treatment compared to vehicle-treated mice (Fig. 1c). However, the effect of a single injection of 4R (1 mg/kg) in cold hypersensitivity,

was transient as responses in 4R-treated animals were indistinguishable from control vehicle-treated mice when tested on days 2 and 7 after 4R treatment. In contrast to the transient effects observed after administration of the lowest dose of 4R, the highest dose of 4R tested (15 mg/kg) resulted in long-lasting decreases in CFA-induced cold hypersensitivity, manifested as significantly ($p < 0.0001$) lower response scores to acetone stimulation of the injected paw, compared to response scores in vehicle-treated mice, in all time-points, tested (Fig. 1c). Administration of 4R at 6 mg/kg of weight resulted in significant ($p < 0.001$) decreases in response scores to acetone stimulation in the CFA-treated hind paw 2–5 h and on day 7 after the single injection of 4R but not on day 2 after treatment. Further analysis revealed that responses to cold stimulation of the injected paw at maximum analgesia (observed 7 days after a single dose of 4R 15 mg/kg) are significantly ($p < 0.01$) higher than responses in the uninjected control paw (Fig. 1c), demonstrating that 4R treatment partially reverses CFA-induced cold allodynia.

Evaluation of CFA-induced hypersensitivity to heat stimuli revealed that 4R also decreases heat hypersensitivity in the inflamed paw in a time and dose-dependent manner (Fig. 1d). Compared to vehicle-treated animals, mice treated with the lowest 4R dose (1 mg/kg), displayed a significant ($p < 0.01$) increase in paw withdrawal latency in response to heat stimulation (less hypersensitivity) of the CFA-injected paw on day 8 (Fig. 1d). At this dose, no effect on CFA-induced thermal hypersensitivity was observed 2–5 h or day 2 after 4R treatment (Fig. 1d). In contrast, administration of the highest dose of 4R (15 mg/kg) showed strong anti-hyperalgesic effects in response to heat stimulation of the injected paw 2–5 h and day 8 ($p < 0.0001$), but not on day 2 after 4R treatment. Furthermore, mice treated with 4R at 6 mg/kg of body weight displayed time-dependent anti-hyperalgesic effects with increasing paw withdrawal latency (less hypersensitivity) compared to vehicle-treated animals as time after treatment progressed. Additional analysis showed no significant differences ($p > 0.05$) in responses to heat stimulation between the uninjected control paw and 4R 6 mg/kg or 15 mg/kg treated CFA-injected paw on day 8 (Fig. 1d). In contrast, paw withdrawal latencies were significantly ($p < 0.0001$) lower 2–5 h after 4R treatment (6 mg/kg and 15 mg/kg) and on day 2 after 4R (6 mg/kg), when compared to the uninjected control paw (Fig. 1d). These results demonstrate that CFA-induced heat hypersensitivity is reversed 8 days after a single dose of 4R treatment (6 mg/kg and 15 mg/kg), but it is only partially reversed by the 1 mg/kg dose at this time-point or after any dose (6 mg/kg and 15 mg/kg) at earlier time-points (2–5 h and day 2).

Lastly, analysis of inflammation-induced hypersensitivity to tactile stimulation revealed a small but statistically significant ($p < 0.05$) increase (less hypersensitivity) in paw withdrawal thresholds in the CFA-injected paw 2–5 h after 4R (1 mg/kg and 15 mg/kg) treatment and 2 days after 4R (1 mg/kg and 6 mg/kg) administration when compared to vehicle-treated mice (Fig. 1e). When compared to the uninjected control paw, paw withdrawal thresholds were significantly ($p < 0.0001$) lower (more hypersensitive) at all time-points and 4R doses evaluated (Fig. 1e). These results indicate that 4R-treated mice are still clearly allodynic, even though there is a very small improvement in their von Frey thresholds.

Notably, measurement of responses to cold, heat, and tactile stimulation of the uninjured hind paw showed that responses in all modalities are indistinguishable in vehicle- and 4R-treated mice throughout the duration of the experiment and independent of the dose tested. These results are significant as they indicate that baseline nociception (in the absence of inflammation) and locomotor responses to peripheral stimuli are unaffected by 4R systemic treatment (Fig. 1c-e). Collectively, these results demonstrate that a single systemic administration of 4R decreases inflammation-induced peripheral hypersensitivity without affecting baseline responses in the uninjured paw.

Systemic 4R administration reduces inflammation-induced thermal but not tactile hypersensitivity in female mice

Previous studies report sex-related mechanistic differences in rodent inflammatory processes that influence nociception and hyperalgesia [56–60]. These findings stress the importance of studying male and female subjects in preclinical pain studies. In line with this, the next set of experiments aimed to determine whether the 4R anti-hyperalgesic effects described above in males are also observed in females using the same experimental approach (Fig. 2a). As illustrated in Fig. 2b-g, evaluation of the responses to acetone, Hargreaves, and von Frey tests showed that female control mice display cold, heat, and tactile hypersensitivity in CFA-injected paws compared to their respective uninjected paws on days 2 and 7 after systemic vehicle treatment. Thus, response scores to acetone stimulation were significantly ($p < 0.01$) higher in CFA-injected hind

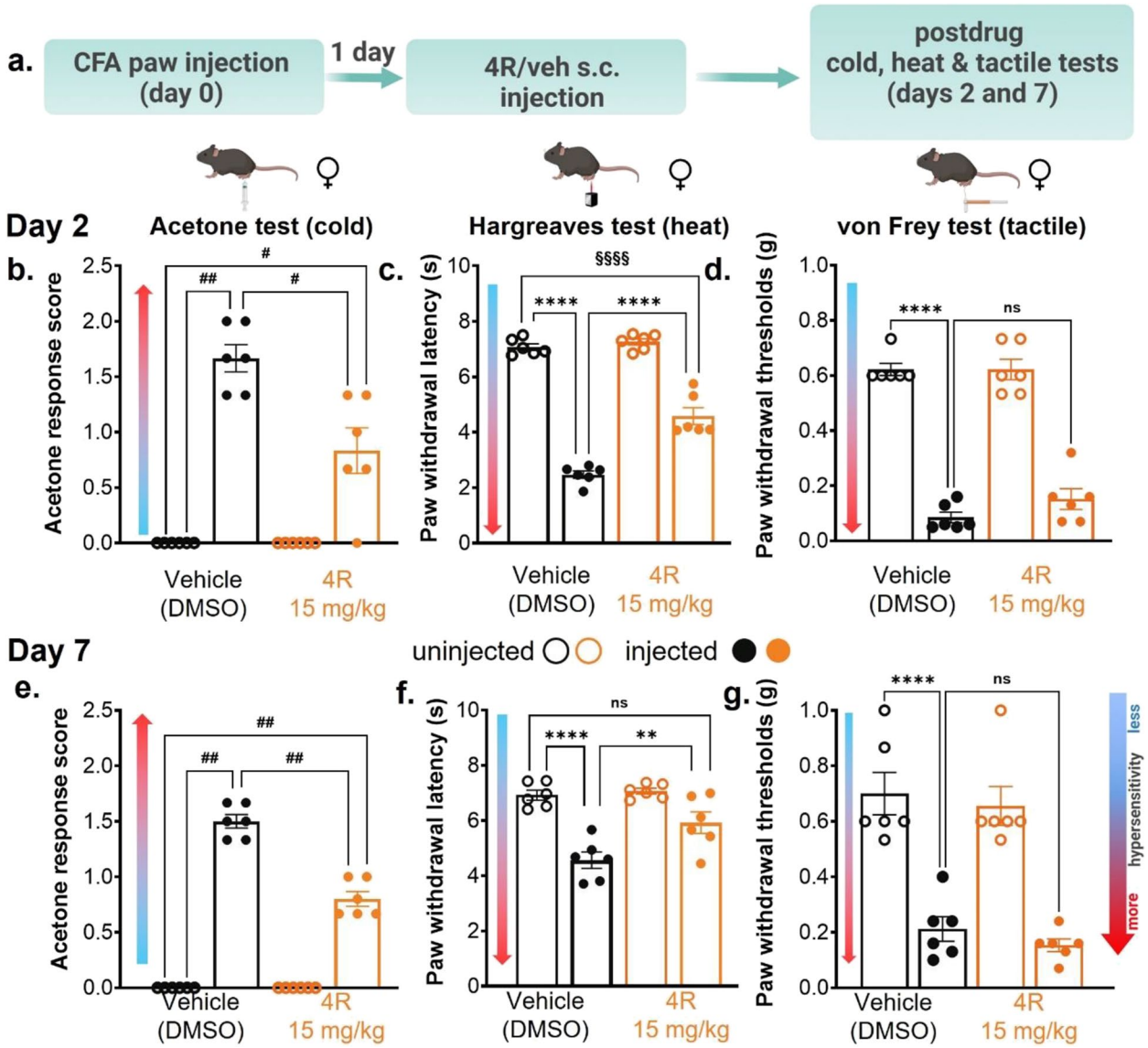

Fig. 2 Systemic 4R administration reduces inflammation-induced thermal but not tactile hypersensitivity in female mice (**a**) Experimental timeline for acetone (cold), Hargreaves (heat) and von Frey (tactile) tests in CFA-injected and uninjected hind paws at days 2 and 7 after 4R (15 mg/kg) or vehicle administration in females. Acetone response score (**b**, **e**), withdrawal latency to heat stimulation (**c**, **f**) and withdrawal threshold to tactile stimulation (**d**, **g**) on experimental days 2 and 7, respectively. All values are expressed as mean ± SEM. $n = 6$ animals per treatment and test. Two-way ANOVA followed by Šídák's multiple comparison test; $p < 0.01$ (**); $p < 0.001$ (***); $p < 0.0001$ (****) or Tukey's multiple comparisons test; adjusted $p < 0.0001$ (§§§§). Mann–Whitney multiple comparisons test, Holm-Šídák method; adjusted $p < 0.05$ (#); adjusted $p < 0.01$ (##). Not significant = ns

paws than in the uninjected hind paws (Fig. 2b, e). Similarly, paw withdrawal latencies and thresholds to heat and tactile stimulation of the CFA-injected paw were significantly ($p < 0.0001$) shorter and lower, respectively, than those measured in the uninjected hind paws (Fig. 2c, d, f, and g).

To investigate the potential effects of 4R in females, we used the 15 mg/kg dose, which consistently reduced inflammation-induced hyperalgesia in males (Fig. 1). These behavioral experiments revealed that a single s.c. injection of 4R (15 mg/kg) in female mice significantly ($p < 0.01$) decreases CFA-induced cold and heat hypersensitivity compared to animals treated with the vehicle on both days 2 and 7 after systemic treatment (Fig. 2b-c, e–f). Thus, on both days tested, response scores to acetone were significantly ($p < 0.05$) lower in the CFA-injected paw of 4R-treated mice than in the injected paws of the vehicle-treated group (Fig. 2b, e). Similarly, paw withdrawal latencies to heat stimulation of the injected paw on both days were significantly ($p < 0.01$) longer in 4R-treated mice than in those treated with vehicle (Fig. 2c, f). Similar to what we observed in males (Fig. 1c-d), CFA-induced heat hypersensitivity was reversed 7 days after a single dose of 4R treatment (15 mg/kg). Thus, there were no significant differences ($p > 0.05$) in responses to heat stimulation between the uninjected control paw, and CFA-injected paw 7 days after 4R (15 mg/kg) treatment (Fig. 2f). In contrast, but also consistent with the male results (Fig. 1c-d), heat hypersensitivity was only partially reversed 2 days after 4R (15 mg/kg) systemic treatment and cold hypersensitivity was partially reversed at all time-points tested in females. Thus, responses to cold stimulation in the CFA-injected paw were significantly ($p < 0.05$) higher on days 2 and 7, and responses to heat stimulation were significantly lower on day 2, after 4R (15 mg/kg) treatment, when compared to the uninjected paw in vehicle condition at the same time-points (Fig. 2b-c, e). In both days tested, sensitivity to cold and heat stimulation of the uninjected hind paw was indistinguishable between vehicle and 4R treated groups.

Evaluation of CFA-induced tactile hypersensitivity in female mice showed that, unlike in males, withdrawal thresholds are comparable in the injected paws of 4R and vehicle-treated mice in both time points evaluated, demonstrating that tactile hypersensitivity is unaltered by 4R treatment (Fig. 2d, g). Similar to the male results, paw withdrawal thresholds in the uninjected hind paws are also indistinguishable in 4R and vehicle-treated female mice, demonstrating that baseline nociception and locomotor responses to peripheral stimuli are unaltered by 4R treatment. Altogether, these findings show that single systemic administration of 4R (15 mg/kg) reduces inflammation-induced thermal but not tactile hypersensitivity in female mice without altering baseline responses.

4R reduces inflammation-induced paw edema in male but not female mice

Previous studies have shown that systemic treatment with 4R has anti-inflammatory effects in the lipopolysaccharide model of inflammation in mice [61]. To test if the 4R anti-hyperalgesic effects described in the sections above are coupled to decreases in inflammation, we evaluated paw thickness as an indirect measurement of inflammation in CFA-injected and uninjected hind paws before and at different time points following the systemic administration of various doses of 4R (1, 6 or 15 mg/kg by body weight) or vehicle (Fig. 3a). As shown in Fig. 3b-c, subcutaneous injection of CFA in the hind paw of control male and female mice (systemically treated with vehicle) resulted in significant ($p < 0.0001$) increases in paw thickness (edema) when compared to their respective uninjected hind paws for the duration of the experiment. Evaluation of paw edema in male mice systemically treated with 4R revealed that a single administration of 4R attenuates inflammation-induced paw edema in a dose and time-dependent manner (Fig. 3b). Thus, male mice treated with the highest (15 mg/kg) and intermediate (6 mg/kg) doses of 4R showed significant ($p < 0.05$) reductions in paw thickness compared to vehicle-treated

(See figure on next page.)

Fig. 3 4R reduces inflammation-induced paw edema in male but not female mice (**a**) Experimental timeline for paw thickness measurements. In vivo thickness measurements of CFA-injected and non-injected hind paws before and 1–8 days after 4R (1, 6, and 15 mg/kg) or vehicle systemic administration of (**b**) male and (**c**) female mice. All values are expressed as mean ± SEM. $n = 6$–16 animals per treatment and sex. Two-way ANOVA (**b**) or Two-way RM ANOVA (**c**) followed by posthoc Tukey's multiple comparisons test: CFA-injected paw vs non-injected paw in pre-drug vehicle (veh) conditions, $p < 0.0001$ (####); 4R CFA-injected paw vs non-injected vehicle conditions day 7, $p < 0.0001$ (§§§§), Two-way ANOVA followed by posthoc Dunnett's multiple comparisons test: vehicle vs 4R systemic treatment in CFA-injected paws of the same time-point, $p < 0.05$ (*), $p < 0.01$ (**) and $p < 0.001$ (***). Results of multiple comparisons between vehicle (veh) and 4R 1 mg/kg, 6 mg/kg or 15 mg/kg are shown in purple, teal and orange asterisks, respectively. (**d**) Experimental timeline for histology samples. **e** Representative H&E images of dermal (D) and subdermal (S) skin, open arrows point to polymorphonuclear immune cell infiltration. Scale Bar: 200 µm. Histological analysis of hind paw skin 8 days post local CFA and 7 days post 4R (**f**) glabrous skin thickness of the hind paws and (**g**) subdermal immune cell count. All values are expressed as mean ± SEM. $n = 5$–6 mice per treatment and sex. Two-way ANOVA followed by Šidák's multiple comparisons test: Vehicle vs 4R, $p < 0.05$ (*), $p < 0.01$ (**)

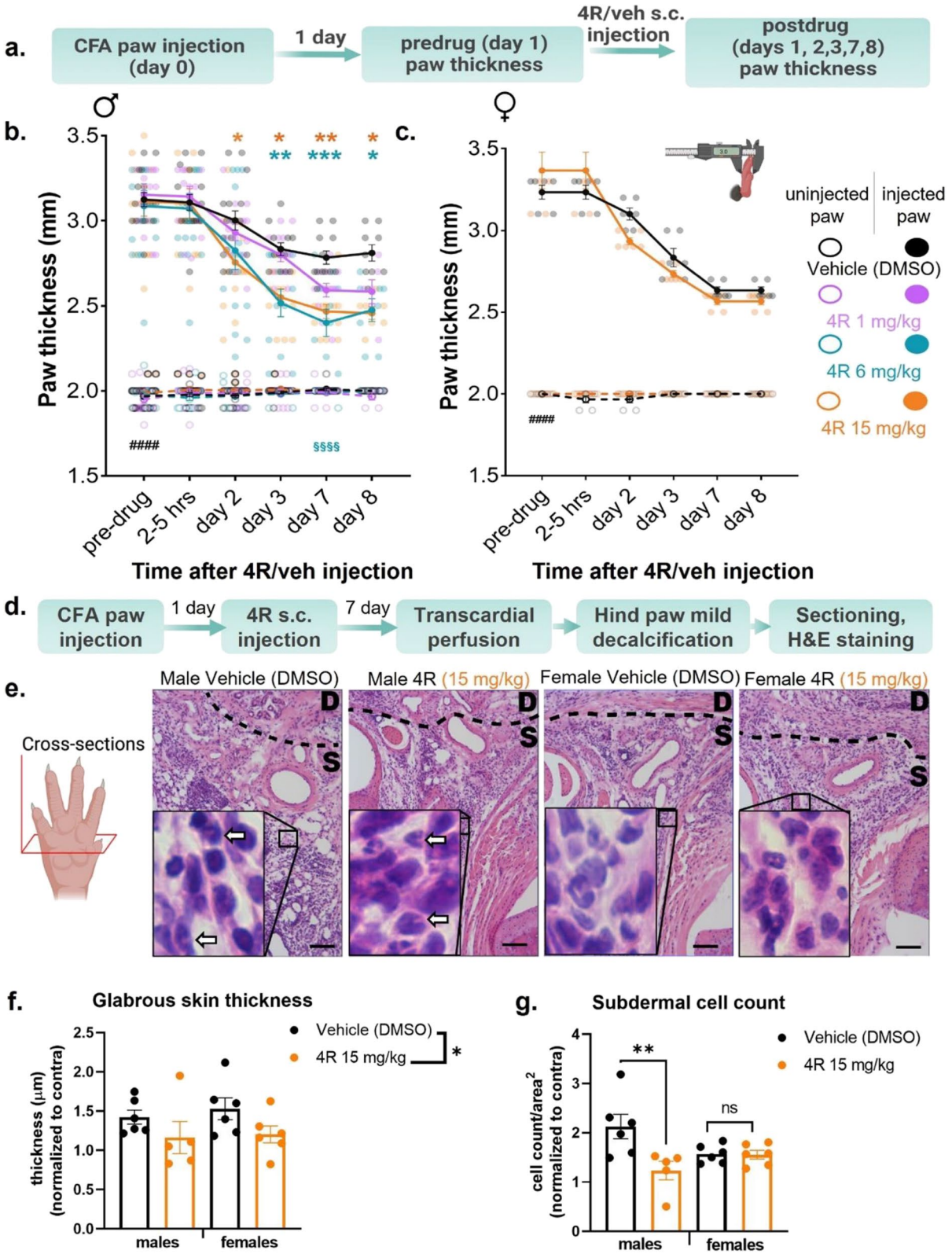

Fig. 3 (See legend on previous page.)

mice. 4R-mediated decreases in CFA-induced paw edema were first observed on day 2 after systemic 4R treatment and lasted for the duration of the experiment (8 days post 4R treatment). In contrast, paw thickness in CFA-injected hind paws of males treated with the lowest dose (1 mg/kg) of 4R was indistinguishable from those measured in vehicle-treated mice at all time points tested. Further analysis showed that paw thickness at the maximum anti-inflammatory effect, measured 7 days after a single dose of 4R (6 mg/kg), is significantly ($p < 0.0001$) higher in the CFA-injected paw, when compared to the uninjected control paw (Fig. 3b), demonstrating that 4R treatment partially reverses the inflammation caused by CFA injection. Importantly, paw thickness in uninjected hind paws were comparable in all treatments independently of dose or time-point, demonstrating that 4R-mediated decreases in paw thickness are specific to the inflamed hind paw.

Parallel experiments were performed to test if 4R-mediated decreases in inflammation-induced paw edema were also observed in female mice. Similar to male mice, female mice also developed paw edema after CFA injection that lasted for the duration of the experiment when compared to the uninjected hind paws ($p < 0.0001$) (Fig. 3c). In marked contrast to the results observed in male mice, however, measurement of CFA-induced paw edema in females after systemic treatment with 4R (15 mg/kg by body weight) were indistinguishable from those in females treated with the vehicle at all time points measured. These results demonstrate that systemic administration of 4R (15 mg/kg by body weight) reduces inflammation-induced paw edema in male but not female mice.

We used a histological approach to further investigate how systemic 4R treatment (15 mg/kg) influenced glabrous skin thickness after CFA injection on day 8 (7 days post-4R treatment) (Fig. 3d-e). Similar to previous studies, there is a robust increase in glabrous skin thickness at 8d post-CFA injection in male and female mice. However, our findings reveal that a single dose of 4R treatment resulted in a significant ($p < 0.05$) reduction in CFA-induced glabrous skin thickness independent of sex (Fig. 3f). In addition to the presence of edema, another hallmark feature of inflammation is a robust increase in immune cell infiltration into the local site of injury. We observed robust subdermal cell counts in the male CFA-injected group. Intervention with systemic 4R 1 day post-CFA injection led to a significant reduction in subdermal cell count in males suggesting an attenuation to the CFA-induced inflammation (Fig. 3g). Evaluating the effect of 4R on immune cell infiltration in female mice showed that the reduction in subdermal cell count occurred independently of 4R treatment revealing that there may be sex-driven differences in the way immune cells respond to 4R treatment (Fig. 3g).

Pretreatment with an α7 nAChRs selective antagonist prevents 4R-induced reductions in inflammation-induced hypersensitivity and paw edema

Previous studies have shown that 4R modulates human nicotinic acetylcholine receptors (nAChRs) [15]. Separate studies have further identified nAChRs, particularly the α7 nAChRs, as potential pharmacological targets for the modulation of pain and inflammation [6, 62, 63]. Based on these combined findings, we hypothesized that the observed 4R-induced decreases in inflammation-induced hypersensitivity and paw edema in mice are mediated via modulation of α7 nAChRs. To test this hypothesis, the α7 nAChRs selective antagonist MLA (10 mg/kg, s.c.) was administered 15 min prior to 4R injection (15 mg/kg, s.c.) in male mice (Fig. 4a). CFA-induced cold and heat hypersensitivity were measured on days 7 and 8 after systemic injections, respectively, corresponding to the time points where we observed higher 4R-mediated anti-hyperalgesic and anti-inflammatory effects (Figs. 1, 2 and 3).

Consistent with the results presented in Fig. 1, animals treated with 4R (15 mg/kg) exhibited lower response scores to acetone stimulation and longer paw withdrawal latencies in response to heat stimulation of the CFA-injected paw compared to vehicle-treated animals, indicating that 4R reduces inflammation-induced cold and heat hypersensitivity (Fig. 4b-c). Evaluation of animals pre-treated with the α7 nAChRs selective antagonist MLA (10 mg/kg) revealed that MLA pretreatment prevents the anti-hyperalgesic effects of 4R (Fig. 4b-c). Consequently, mice systemically treated with MLA prior to 4R show significantly ($p < 0.01$) higher response scores to acetone stimulation (Fig. 4b) and significantly ($p < 0.01$) shorter paw withdrawal latencies in response to heat stimulation (Fig. 4c) of the CFA-injected paw compared with responses measured in animals pre-treated with MLA vehicle followed by 4R. Analysis of CFA-induced paw edema further revealed that, consistent with the results shown in Fig. 3b, a single injection of 4R (15 mg/kg) significantly ($p < 0.05$) reduced CFA-induced paw edema starting at day 2 post 4R treatment when compared to vehicle-injected male mice (Fig. 4d). Pretreatment with MLA (10 mg/kg) prevented the 4R-mediated reductions in paw thickness at days 7 and 8 after treatment. Importantly, CFA-induced thermal hypersensitivity and paw edema were not measurably affected by administration of MLA in the absence of 4R compared to vehicle-treated mice, demonstrating that systemic administration of the α7 nAChRs selective antagonist MLA does not measurably affect responses to cold or heat stimulation or CFA-induced paw edema (Fig. 4b-d).

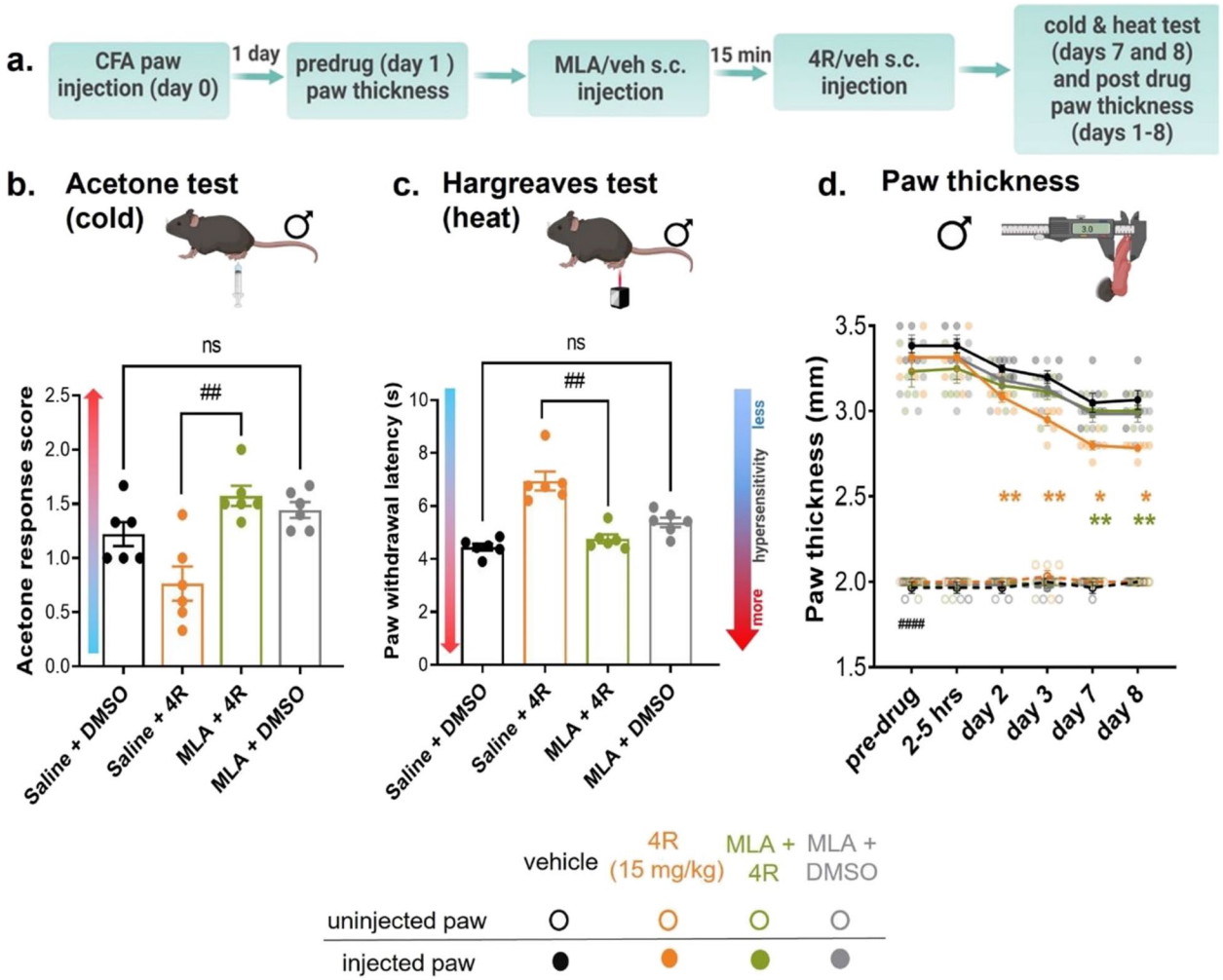

Fig. 4 Pretreatment with an α7 nAChRs selective antagonist prevents 4R-induced reductions in inflammation-induced hypersensitivity and paw edema (**a**) Experimental timeline. CFA-injected and non-injected paw thickness measurements were taken in pre-drug condition. One day after CFA paw injection, MLA (10 mg/kg) or vehicle (veh) was systemically administered and 15 min after, animals received 4R (15 mg/kg) or veh treatment (s.c.). CFA-injected and non-injected paw thickness was measured 1–8 days after 4R (15 mg/kg), MLA (10 mg/kg) or vehicle administration. Acetone (cold) and Hargreaves (heat) tests in CFA-injected and non-injected hind paws were performed 7–8 days after systemic drug administration. (**b**, **c**) Acetone response scores (**b**) and paw withdrawal latencies in response to heat stimulation (**c**); Kruskal–Wallis test followed by posthoc Dunn's multiple comparison test; saline + 4R vs. MLA + 4R; $p < 0.01$ (##); saline + DMSO vs. MLA + DMSO, $p > 0.05$, not significant (ns). (**d**) Thickness measurements of CFA-injected and non-injected hind paws; Two-way RM ANOVA followed by posthoc Tukey's multiple comparisons test: CFA-injected paw vs uninjected paw in pre-drug veh conditions, $p < 0.0001$ (####). Two-way RM ANOVA followed by posthoc Tukey's multiple comparisons test: CFA-injected paws in saline + DMSO vs saline + 4R systemic treatments and MLA + 4R vs saline + 4R at the same time-point, $p < 0.05$ (*), $p < 0.01$ (**). All values are expressed as mean ± SEM. $n = 6$ animals per treatment and test

Collectively, these results demonstrate that 4R-induced reductions in inflammation-induced hypersensitivity and paw edema are mediated by positive modulation of α7 nicotinic acetylcholine receptors.

α7 nAChRs are expressed on a subset of subdermal macrophages but are not upregulated after CFA or 4R treatment

Due to the previously described role of macrophages in the innate immune responses [64–66], we hypothesized that α7 nAChRs $^{+}$ macrophages might play a role in analgesia and resolving inflammation and are modulated after 4R treatment in Iba1^{+} macrophages. However, when colocalizing α7^{tdT+} and Iba1^{+} cells, we found no significant changes to normalized cell count in the subdermal region of the hind paw at day 8 post-CFA (Fig. 5a-e). We also wanted to determine if α7^{tdT}nAChRs overlapped with CD3^{+} T-cells and F4/80^{+} macrophages in whole skin and performed flow cytometry on dissociated hind paw skin from CFA-treated (ipsi) and non-treated

(contra) male and female animals. Similar to the above IHC experiment, we did not observe a significant change in $\alpha7^{tdT+}$ cells after CFA but found roughly 7% of dissociated cells were $\alpha7^{tdT+}$ and close to 20% of these cells are $F4/80^{+}$ macrophages and 10% are $CD3^{+}$ T-cells (Fig. 5f-h).

Discussion

The link between tobacco and pain has been known for decades [3]. However, its potential to treat pain is hindered by the harmful and highly addictive properties associated with tobacco use. The potential function of other components of the tobacco plant for pain treatment is understudied. In the present study, we investigated whether systemic administration of the 4R tobacco cembranoid results in anti-inflammatory effects and pain relief in a mouse model of inflammatory pain. Our findings demonstrate that systemic administration of 4R reduces peripheral hyperalgesia in both male and female mice. We further show that 4R reduces inflammation-induced paw edema and hind paw subdermal immune cell infiltration in males but not females, supporting the growing body of evidence demonstrating that modulation of pain and inflammatory responses is sexually dimorphic [57, 58, 60, 67]. Notably, our experiments demonstrate that 4R-mediated analgesia and anti-inflammatory effects last up to 8d after a single systemic administration, highlighting its potential therapeutical use in reducing persistent inflammation and pain. Lastly, using a pharmacological approach, our behavioral experiments show that 4R-mediated reductions in peripheral hyperalgesia and inflammation-induced paw edema are driven by the modulation of nicotinic receptors, particularly the α7 nAChRs. Altogether, our findings identify the 4R tobacco cembranoid as an analgesic and anti-inflammatory agent and further support targeting the cholinergic system for pain and inflammation treatment.

4R-mediated anti-hyperalgesic and anti-inflammatory effects are sexually dimorphic

Our behavioral experiments using the CFA model of inflammatory pain show that a single systemic administration of 4R reduces inflammation-induced heat hypersensitivity in both male and female mice (Figs. 1d and 2c). However, we also show that 4R-mediated reductions in inflammation-induced tactile and cold hypersensitivity, albeit modest, are only observed in males but not females, despite the robust inflammation-induced hypersensitivity seen in both sexes (Figs. 1c, e and 2b, d). Similarly, systemic treatment with 4R results in reductions in inflammation-induced paw edema in males but has no effect in females despite the robust inflammation-induced paw edema elicited in both sexes (Fig. 3). Collectively, these results demonstrate that 4R-mediated anti-hyperalgesic and anti-inflammatory effects are sexually dimorphic, increasing the evidence in support of distinct mechanisms for inflammation and pain processing in males and females [57, 58, 60] and stressing the importance of incorporating both sexes in preclinical studies.

An important caveat of our studies is that we only evaluated one 4R dose (15 mg/kg) in females, whereas a full dose response was performed in male mice. We selected this dose for the female experiments because it consistently reduced inflammation-induced hyperalgesia and paw edema in males. This concern is mitigated by the similarities in the 4R-mediated anti-hyperalgesic effects observed in males and females. It suggests that the lack of measurable effect in paw edema in females is not due to the experimental dose selected. Given that previous studies evaluating the pharmacokinetics and metabolism of 4R in vivo have only been performed in male rats [45], future experiments to address potential sex differences in 4R drug activity are needed.

Anti-hyperalgesic and anti-inflammatory effects after a single systemic dose of 4R are prolonged

Previous pharmacokinetic and metabolic experiments have shown that the half-life of 4R, when administered systemically in rats, is between 36 min to 1.5 h [45]. These studies further showed no measurable plasma (or brain) levels of 4R 8 h post-administration. Consistent with the reported pharmacokinetics of 4R, our behavioral experiments show 4R-mediated anti-hyperalgesic effects 2.5 h after a single systemic 4R administration (Fig. 1). Notably,

(See figure on next page.)

Fig. 5 α7 nAChRs expression in hind paw macrophages (**a**) Experimental Timeline. Immunohistochemistry of $\alpha7^{tdT}$/$Iba1^{+}$ macrophages in CFA-injected and non-injected hind paw skin (subdermal) 8 days post-CFA (day 0) and 7 days post 4R (15 mg/kg) or veh treatment (s.c.) (day 8). (**b**) A representative image of $\alpha7^{tdT}$ and $Iba1^{+}$ hind paw subdermal co-expression. Scale bar: 20 µm. **c** Cell counts normalized to the area of subdermal $\alpha7^{tdT}$ cells. (**d**) Cell counts normalized to the area of subdermal Iba1 + cells. (**e**) Cell counts normalized of colocalized $\alpha7^{tdT}$ and $Iba1^{+}$. (**f**) Experimental Timeline. Flow cytometric analysis of hind paw subdermal macrophages (F4/80) and T-cells (CD3) of CFA-injected (ipsi) and non-injected (contra) hind paw skin 8 days post-CFA only. (**g**) Hind paw skin was enzymatically dissociated and stained with F4/80, CD3, and endogenous $\alpha7^{tdT}$. After gating for dissociated hind paw skin cells based on forward and side scatter, cells were differentiated by their $tdTomato^{+}$ signal, then subdivided into F4/80 and CD3 populations. (**h**) Analysis of overlapping of $tdTomato^{+}$ cells that are either macrophages or T-cells in males and females

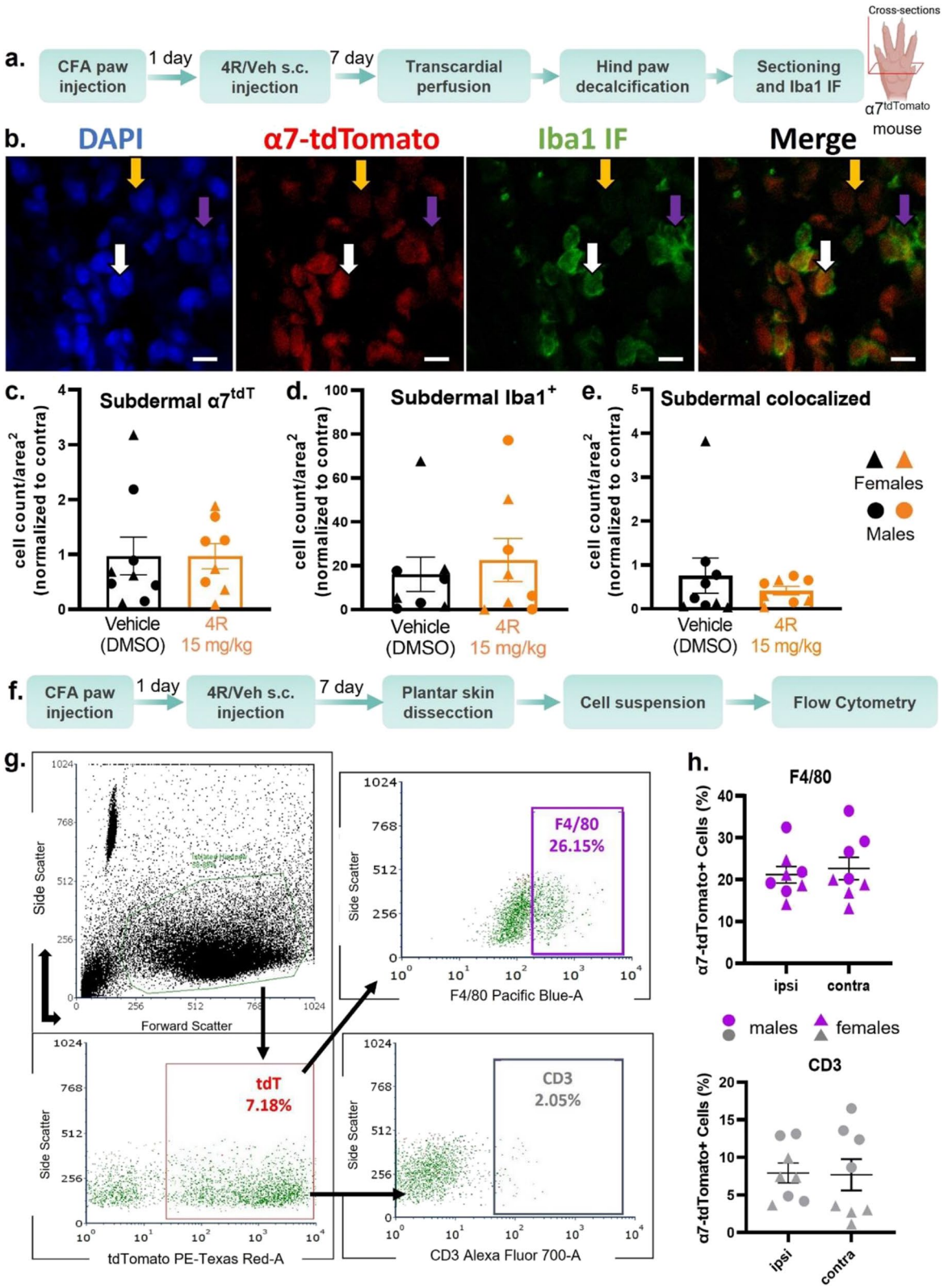

Fig. 5 (See legend on previous page.)

however, our behavioral time course further showed that 4R anti-hyperalgesic effects are long-lasting, with robust effects measured up to 8 days after administration of a single dose of 4R (Figs. 1 and 2). These results show that the behavioral effects of a single dose of 4R are persistent, outlasting the half-life of 4R, and present at time points when 4R is no longer measurably detected in the plasma or brain [45] (Fig. 6).

It is important to note that 4R effects are restricted to the inflamed paw, as no measurable effect was observed in the uninflamed paw. These results highlight that 4R treatment does not alter baseline sensory and locomotor responses to noxious stimulation, an evolutionary function essential for survival. These findings are also consistent with previous studies in rats that demonstrate that locomotor activity is not affected by systemic 4R administration [15]. A significant translational consideration in future studies is whether 4R produces dependence or addiction, as has been reported with other commonly used treatments for pain such as opioids [69]. This is particularly important given that 4R has been shown to bind to and modulate α4β2 nAChRs [15, 28], which have been previously linked to nicotine addiction [70, 71]. However, these concerns are mitigated by studies demonstrating that 4R reduces nicotine-induced withdrawal-like effects in planarians [72] and blocks behavioral sensitization to nicotine in rats [15]. Whether 4R treatment at the doses and time-points used in the present study are rewarding and potentially addictive, remains unknown and will be important to determine in the future.

At the inflammatory level, our results show that 4R-mediated decreases in inflammation-induced paw edema are delayed and not detected until 2 days post systemic 4R treatment (Fig. 3), when 4R is no longer detected in the body [45] (Fig. 6). Similar to the behavioral effects, the anti-inflammatory effects of a single dose of 4R are also persistent, with decreases in paw edema measured up to 8 days after administration of a single dose (Fig. 3). An important caveat of these experiments is that paw edema is an indirect gross measurement of inflammation and is limited by the sensitivity of the assay. Therefore, experiments to determine the effects of 4R in inflammatory responses at microscopic, cellular, and biochemical levels are warranted. Nonetheless, our findings demonstrate that 4R-mediated anti-inflammatory effects persist after the drug is eliminated from the body.

Altogether, our experiments show that 4R anti-inflammatory and anti-hyperalgesic effects outlast drug duration in the body (Fig. 6), suggesting that 4R effects occur via modulation of downstream signaling pathways. An alternative explanation is that a single dose of 4R administered shortly after injury interferes with the inflammatory response and subsequent development of persistent inflammation and hypersensitivity. Potential effects in central and/or peripheral nervous systems independent of the inflammatory response are also possible. Whether the anti-inflammatory and anti-hyperalgesic effects of 4R depend on the timing of drug administration relative to injury remains to be elucidated. Previous experiments have shown, for example, that systemic 4R treatment administered before and after brain injury in rats reduces neuronal death and inflammation [25]. Thus, it will be informative to know if systemic administration of 4R prior to injury also prevents the development of peripheral inflammation and hypersensitivity in mice, which could have important applications in preemptive analgesia. Determining the effects of 4R when administrated at later time points following injury will also be necessary. Lastly, longitudinal studies are also needed to determine if 4R treatment results in faster injury-induced inflammation and hyperalgesia recovery.

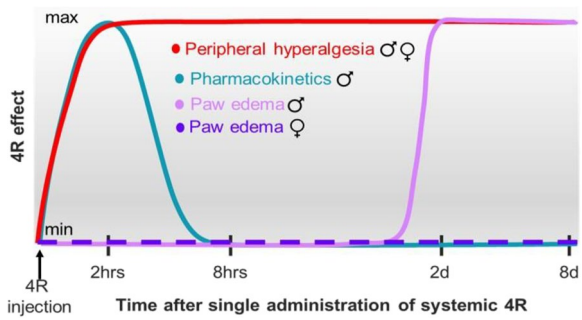

Fig. 6 4R effects as a function of time. (**a**) Diagram of 4R effects in males and females as a function of time. Effects on peripheral hyperalgesia (red line) and paw edema (pink line for males and purple line for females) are shown relative to previously published pharmacokinetics [68] (blue line)

4R reduces pain and inflammation via modulation of α7 nAChRs

Our experiments demonstrate that systemic administration of the tobacco cembranoid 4R reduces inflammation-induced hypersensitivity and paw edema (Figs. 1, 2 and 3). Using pharmacological approaches, we further show that pretreatment with MLA, a selective α7 nAChRs antagonist, prevents 4R-mediated anti-hyperalgesic and anti-inflammatory effects (Fig. 4). Together, these results demonstrate that the anti-hyperalgesic and anti-inflammatory effects of 4R are mediated via positive modulation of α7 nAChRs. Our findings are consistent with a large body of literature demonstrating that positive modulation of α7 nAChRs is analgesic and anti-inflammatory [63]. Previous studies in animal pain models, for example, have shown that pharmacological

modulation of these receptors has anti-inflammatory, anti-allodynic, and anti-hyperalgesic effects that have also been associated with the downregulation of cytokine levels and inflammatory pathways [48, 73, 74]. Moreover, past studies have demonstrated that α7 knockout mice display increases in hyperalgesia, paw edema, and allodynia compared to wild type mice in the CFA model of inflammatory pain, while baseline responses to noxious stimulation are comparable between α7 knockout and wild type mice [55]. These findings suggest that α7 nAChRs contribute to an endogenous analgesic tone during persistent inflammation.

α7 nAChRs are expressed on a subset of subdermal macrophages but are not upregulated after CFA or 4R treatment

Our findings show that the systemic administration of 4R elicits a male-specific reduction of hind paw subdermal immune cells, which parallels the reduction of edema seen in males. This sexually dimorphic anti-inflammatory effect of 4R adds to increasing evidence of the existence of sex-specific mechanisms in pain and inflammation [75]. It does not appear that local macrophages play a role in the observable α7 nAChRs mediated anti-inflammatory effects. We were unable to observe a significant change of $\alpha7^{tdTomato}/Iba1^{+}$ colocalized cell populations (Fig. 5a-e). This suggests there is another major cell population that is contributing to the attenuation of the CFA-induced inflammatory pain model after 4R treatment. It is known that other immune cells infiltrate the skin after CFA treatment. In addition to the expression on macrophages and T-cells, α7 nAChRs are also expressed on, B-cells, neutrophils, mast cells [34, 76, 77]. Future studies are needed to evaluate the contribution of other α7 nAChRs-expressing immune cell types in 4R modulation of pain-related behaviors and inflammation to further our understanding of cellular mechanisms.

An important factor to consider in the interpretation of our pharmacological experiments is that MLA has been previously shown to bind, albeit to a much lower affinity, to α9α10 nAChRs [78]. Given that the reported relative affinity of MLA is much higher for α7 nAChRs than for α9α10 nAChRs [78–81], it is most likely that the anti-hyperalgesic and anti-inflammatory effects we see here are mediated via modulation of α7 nAChRs.

The results from our in vivo pharmacological experiments showing that 4R effects are mediated via α7 nAChRs, along with previous studies in vitro demonstrating that 4R can also bind α4β2, α3β4, and α1β1γδ nAChRs [15, 28], confirm that 4R can modulate multiple nicotinic receptors. It is important to note that, to the best of our knowledge, 4R is not known to bind to or directly modulate α7 nAChRs. Future studies to evaluate whether 4R binds to and directly modulates α7 nAChRs are needed. Studies have shown, however, that multiple cholinergic receptors are expressed in different tissues and cell types contributing to neuroimmune responses [82]. It is therefore possible that 4R modulates α7 nAChRs via an indirect mechanism that does not require direct binding to the receptor. For example, 4R may bind to and modulate a different type of cholinergic receptor within the endogenous cholinergic anti-inflammatory pathway, which subsequently leads to indirect modulation of α7 nAChRs, ultimately decreasing inflammation and behavioral hypersensitivity. Determination of the relative affinity of 4R to different nicotinic receptors and further characterization of the mechanism of action of 4R in distinct targets are essential. Nonetheless, the beneficial effects of 4R treatment presented here, along with the neuroprotective, anti-tumor, anti-inflammatory, and antimicrobial effects reported in previous studies [17, 19, 20, 23, 27, 28, 83] suggest that 4R can non-selectively activate tissue and pathological state-specific cell signaling cascades downstream from neural and/or immune nicotinic receptors, improving diverse pathological states, including pain.

Abbreviations

4R	[(1S, 2E, 4R, 6R, 7E, 11E)-cembra-2,7,11-triene-4,6-diol]
CFA	Complete Freund's Adjuvant
DMSO	Dimethyl sulfoxide
MLA	Methyllycaconitine
nAChRs	Nicotinic acetylcholine receptors
s.c.	Subcutaneous
α7 nAChRs	Alpha7 nicotinic acetylcholine receptors
IHC	Immunohistochemistry
NIH	National Institutes of Health
NMR	Nuclear Magnetic Resonance
TLC	Thin layer chromatography
PBS	Phosphate-buffered saline
4% PFA/PB	4% Paraformaldehyde in phosphate-buffered saline solution
H&E	Hematoxylin and eosin
NGS	Normal goat serum
BSA	Bovine serum albumin
Iba1	Ionized calcium-binding adaptor molecule 1
$\alpha7^{tdT+}$	$TdTomato^{+}$ cre driven nAChRs
S.E.M.	Standard error of the mean

Supplementary Information

The online version contains supplementary material available at https://doi.org/10.1186/s12950-023-00373-8.

Additional file 1. Raw Data Table.

Acknowledgements

We thank Dr. Sudhuman Singh for his training and assistance with the behavioral experiments. We thank Phuoc Pham and George Dold (NIH Section on Instrumentation) for help designing and fabricating the custom-built instruments used in this study. Graphics in figures were created with BioRender.com.

Authors' contributions
Conceptualization, L.G.R.G, V.E., P.F., Y.C., M.D.B.; Investigation, L.G.R.G., A.M.F.M, T.D.W. Z.W.C., C.D.U., M.D.B.; Data Analysis, L.G.R., A.M.F.M, C.D.U., M.D.B., Y.C.; Writing, L.G.R.G, P.F., A.M.F.M., M.D.B., Y.C.; Supervision, Y.C., M.D.B.; Funding Acquisition, Y.C., M.D.B.

Funding
This research was supported by the National Center for Complementary and Integrative Health and the National Institute of Neurological Disorders and Stroke Intramural Research Programs (Y.C.). The National Institute of General Medical Sciences Extramural Research Program (grant numbers GM147094 and DK130015) (M.D.B), the University of Texas System Rising STARS program (M.D.B).

Availability of data and materials
All data in this study is available from the corresponding author.

Declarations

Competing interests
The authors declare no competing interests.

Author details
[1]Division of Intramural Research National Center for Complementary and Integrative Health, 35 Convent Drive, Building 35A / Room 1E-410, Bethesda, MD 20892, USA. [2]Department of Neuroscience, Universidad Central Del Caribe School of Medicine, Bayamon, Puerto Rico, USA. [3]Neuroimmunology and Behavior Group, Department of Neuroscience, Center for Advanced Pain Studies (CAPS), School of Behavioral and Brain Sciences, University of Texas, Dallas, USA. [4]National Institute On Drug Abuse, National Institutes of Health, 35 Convent Drive, Building 35A / Room 1E-410, Bethesda, MD 20892, USA.

Received: 5 September 2023 Accepted: 21 December 2023
Published online: 24 January 2024

References

1. Sanchez-Ramos JR. The rise and fall of tobacco as a botanical medicine. J Herb Med. 2020;22:100374.
2. Berlowitz I, Torres EG, Walt H, Wolf U, Maake C, Martin-Soelch C. "Tobacco Is the Chief Medicinal Plant in My Work": Therapeutic Uses of Tobacco in Peruvian Amazonian Medicine Exemplified by the Work of a Maestro Tabaquero. Front Pharmacol. 2020;11:594591.
3. Charlton A. Medicinal uses of tobacco in history. J R Soc Med. 2004;97(6):292–6.
4. Maehle AH. "Receptive substances": John Newport Langley (1852–1925) and his path to a receptor theory of drug action. Med Hist. 2004;48(2):153–74.
5. Miwa JM, Freedman R, Lester HA. Neural systems governed by nicotinic acetylcholine receptors: emerging hypotheses. Neuron. 2011;70(1):20–33.
6. Hone AJ, McIntosh JM. Nicotinic acetylcholine receptors in neuropathic and inflammatory pain. FEBS Lett. 2018;592(7):1045–62.
7. Rosas-Ballina M, Olofsson PS, Ochani M, Valdes-Ferrer SI, Levine YA, Reardon C, et al. Acetylcholine-Synthesizing T Cells Relay Neural Signals in a Vagus Nerve Circuit. Science. 2011;334(6052):98–101.
8. Wang H, Yu M, Ochani M, Amella CA, Tanovic M, Susarla S, et al. Nicotinic acetylcholine receptor alpha 7 subunit is an essential regulator of inflammation. Nature. 2003;421(6921):384–8.
9. Gautron L, Rutkowski JM, Burton MD, Wei W, Wan Y, Elmquist JK. Neuronal and nonneuronal cholinergic structures in the mouse gastrointestinal tract and spleen. J Comp Neurol. 2013;521(16):3741–67.
10. Dhanasobhon D, Medrano MC, Becker LJ, Moreno-Lopez Y, Kavraal S, Bichara C, et al. Enhanced analgesic cholinergic tone in the spinal cord in a mouse model of neuropathic pain. Neurobiol Dis. 2021;155:105363.
11. Chiari A, Tobin JR, Pan HL, Hood DD, Eisenach JC. Sex differences in cholinergic analgesia I: a supplemental nicotinic mechanism in normal females. Anesthesiology. 1999;91(5):1447–54.
12. Chen SR, Pan HL. Spinal GABAB receptors mediate antinociceptive actions of cholinergic agents in normal and diabetic rats. Brain Res. 2003;965(1–2):67–74.
13. Omare MO, Kibet JK, Cherutoi JK, Kengara FO. A review of tobacco abuse and its epidemiological consequences. J Public Health. 2022;30:1485–500.
14. Saito Y, Takizawa H, Konishi S, Yoshida D, Mizusaki S. Identification of cembratriene-4,6-diol as antitumor-promoting agent from cigarette smoke condensate. Carcinogenesis. 1985;6(8):1189–94.
15. Ferchmin P, Lukas R, Hann R, Fryer J, Eaton J, Pagan O, et al. Tobacco cembranoids block behavioral sensitization to nicotine and inhibit neuronal acetylcholine receptor function. J Neurosci Res. 2001;64(1):18–25.
16. Roberts DL, Rowland RL. Macrocyclic Diterpenes. a- and /3–4,8,13-Duvatriene-l,3-diols from Tobacco. J Org Chem. 1962;27(11):3989–95.
17. Yan N, Du Y, Liu X, Zhang H, Liu Y, Zhang Z. A Review on Bioactivities of Tobacco Cembranoid Diterpenes. Biomolecules. 2019;9(1):30.
18. Mudhish EA, Siddique AB, Ebrahim HY, Abdelwahed KS, King JA, El Sayed KA. The Tobacco beta-Cembrenediol: A prostate cancer recurrence suppressor lead and prospective scaffold via modulation of indoleamine 2,3-dioxygenase and tryptophan dioxygenase. Nutrients. 2022;14(7):1505.
19. Fu H, Wang J, Wang J, Liu L, Jiang J, Hao J. 4R-cembranoid protects neuronal cells from oxygen-glucose deprivation by modulating microglial cell activation. Brain Res Bull. 2022;179:74–82.
20. Martins AH, Hu J, Xu Z, Mu C, Alvarez P, Ford BD, et al. Neuroprotective activity of (1S,2E,4R,6R,-7E,11E)-2,7,11-cembratriene-4,6-diol (4R) in vitro and in vivo in rodent models of brain ischemia. Neuroscience. 2015;291:250–9.
21. Eterovic VA, Del Valle-Rodriguez A, Perez D, Carrasco M, Khanfar MA, El Sayed KA, et al. Protective activity of (1S,2E,4R,6R,7E,11E)-2,7,11-cembratriene-4,6-diol analogues against diisopropylfluorophosphate neurotoxicity: preliminary structure-activity relationship and pharmacophore modeling. Bioorg Med Chem. 2013;21(15):4678–86.
22. Eaton MJ, Ospina CA, Rodriguez AD, Eterovic VA. Differential inhibition of nicotine- and acetylcholine-evoked currents through alpha4beta2 neuronal nicotinic receptors by tobacco cembranoids in Xenopus oocytes. Neurosci Lett. 2004;366(1):97–102.
23. Ferchmin PA, Hao J, Perez D, Penzo M, Maldonado HM, Gonzalez MT, et al. Tobacco cembranoids protect the function of acute hippocampal slices against NMDA by a mechanism mediated by alpha4beta2 nicotinic receptors. J Neurosci Res. 2005;82(5):631–41.
24. Eterovic VA, Perez D, Martins AH, Cuadrado BL, Carrasco M, Ferchmin PA. A cembranoid protects acute hippocampal slices against paraoxon neurotoxicity. Toxicol In Vitro. 2011;25(7):1468–74.
25. Ferchmin PA, Andino M, Reyes Salaman R, Alves J, Velez-Roman J, Cuadrado B, et al. 4R-cembranoid protects against diisopropylfluorophosphate-mediated neurodegeneration. Neurotoxicology. 2014;44:80–90.
26. Ferchmin PA, Perez D, Cuadrado BL, Carrasco M, Martins AH, Eterovic VA. Neuroprotection against diisopropylfluorophosphate in acute hippocampal slices. Neurochem Res. 2015;40(10):2143–51.
27. Olsson E, Holth A, Kumlin E, Bohlin L, Wahlberg I. Structure-related inhibiting activity of some tobacco cembranoids on the prostaglandin synthesis in vitro. Planta Med. 1993;59(4):293–5.
28. Ferchmin PA, Pagan OR, Ulrich H, Szeto AC, Hann RM, Eterovic VA. Actions of octocoral and tobacco cembranoids on nicotinic receptors. Toxicon. 2009;54(8):1174–82.
29. Zhu S, Huang S, Xia G, Wu J, Shen Y, Wang Y, et al. Anti-inflammatory effects of alpha7-nicotinic ACh receptors are exerted through interactions with adenylyl cyclase-6. Br J Pharmacol. 2021;178(11):2324–38.
30. Hone AJ, McIntosh JM. Nicotinic acetylcholine receptors in neuropathic and inflammatory pain. FEBS Lett. 2018;592(7):1045–62.
31. Umana IC, Daniele CA, McGehee DS. Neuronal nicotinic receptors as analgesic targets: It's a winding road. Biochem Pharmacol. 2013;86(8):1208–14.
32. Wu YJ, Wang L, Ji CF, Gu SF, Yin Q, Zuo J. The role of alpha7nAChR-mediated cholinergic anti-inflammatory pathway in immune cells. Inflammation. 2021;44(3):821–34.
33. Umana IC, Daniele CA, Miller BA, Abburi C, Gallagher K, Brown MA, et al. Nicotinic modulation of descending pain control circuitry. Pain. 2017;158(10):1938–50.

34. Kageyama-Yahara N, Suehiro Y, Yamamoto T, Kadowaki M. IgE-induced degranulation of mucosal mast cells is negatively regulated via nicotinic acetylcholine receptors. Biochem Biophys Res Commun. 2008;377(1):321–5.
35. de Lucas-Cerrillo AM, Maldifassi MC, Arnalich F, Renart J, Atienza G, Serantes R, et al. Function of partially duplicated human α77 nicotinic receptor subunit CHRFAM7A gene: potential implications for the cholinergic anti-inflammatory response. J Biol Chem. 2011;286(1):594–606.
36. Pavlov VA, Tracey KJ. Controlling inflammation: the cholinergic anti-inflammatory pathway. Biochem Soc Trans. 2006;34(6):1037–40.
37. Fujii YX, Fujigaya H, Moriwaki Y, Misawa H, Kasahara T, Grando SA, et al. Enhanced serum antigen-specific IgG1 and proinflammatory cytokine production in nicotinic acetylcholine receptor alpha7 subunit gene knockout mice. J Neuroimmunol. 2007;189(1–2):69–74.
38. Kimura K, Inaba Y, Watanabe H, Matsukawa T, Matsumoto M, Inoue H. Nicotinic alpha-7 acetylcholine receptor deficiency exacerbates hepatic inflammation and fibrosis in a mouse model of non-alcoholic steatohepatitis. J Diabetes Investig. 2019;10(3):659–66.
39. Bagdas D, Sonat FA, Hamurtekin E, Sonal S, Gurun MS. The antihyperalgesic effect of cytidine-5′-diphosphate-choline in neuropathic and inflammatory pain models. Behav Pharmacol. 2011;22(5–6):589–98.
40. Loram LC, Taylor FR, Strand KA, Maier SF, Speake JD, Jordan KG, et al. Systemic administration of an alpha-7 nicotinic acetylcholine agonist reverses neuropathic pain in male Sprague Dawley rats. J Pain. 2012;13(12):1162–71.
41. Hurst JL, West RS. Taming anxiety in laboratory mice. Nature Methods. 2010;7(10):825–6.
42. Festing MF, Altman DG. Guidelines for the design and statistical analysis of experiments using laboratory animals. ILAR J. 2002;43(4):244–58.
43. Guo Y, Logan HL, Glueck DH, Muller KE. Selecting a sample size for studies with repeated measures. BMC Med Res Methodol. 2013;13:100.
44. Dell RB, Holleran S, Ramakrishnan R. Sample size determination. ILAR J. 2002;43(4):207–13.
45. Vélez-Carrasco W, Green CE, Catz P, Furimsky A, O'Loughlin K, Eterović VA, et al. Pharmacokinetics and Metabolism of 4R-Cembranoid. PLoS One. 2015;10(3):e0121540-e.
46. Nair A, Jacob S. A simple practice guide for dose conversion between animals and human. J Basic Clin Pharm. 2016;7(2):27-.
47. Freitas K, Negus SSS, Carroll FI, Damaj MI. In vivo pharmacological interactions between a type II positive allosteric modulator of α7 nicotinic ACh receptors and nicotinic agonists in a murine tonic pain model. Br J Pharmacol. 2013;169(3):567–79.
48. El Nebrisi EG, Bagdas D, Toma W, Al Samri H, Brodzik A, Alkhlaif Y, et al. Curcumin acts as a positive allosteric modulator of α 7 -nicotinic acetylcholine receptors and reverses nociception in mouse models of inflammatory pain. J Pharmacol Exp Ther. 2018;365(1):190–200.
49. Wilson TDTD, Valdivia S, Khan A, Ahn HSHS, Adke APAP, Gonzalez SM, et al. Dual and opposing functions of the central amygdala in the modulation of pain. Cell Reports. 2019;29(2):332–46.e5.
50. Yoon C, Wook YY, Sik NH, Ho KS, Mo CJ. Behavioral signs of ongoing pain and cold allodynia in a rat model of neuropathic pain. Pain. 1994;59(3):369–76.
51. Colburn RW, Lubin ML, Stone DJ Jr, Wang Y, Lawrence D, D'Andrea MR, et al. Attenuated cold sensitivity in TRPM8 null mice. Neuron. 2007;54(3):379–86.
52. El Sayed KA, Laphookhieo S, Yousaf M, Prestridge JA, Shirode AB, Wali VB, et al. Semisynthetic and biotransformation studies of (1S,2E,4S,6R,7E,11E)-2,7,11-cembratriene-4,6-diol. J Nat Prod. 2008;71(1):117–22.
53. Medhurst SJ, Hatcher JP, Hille CJ, Bingham S, Clayton NM, Billinton A, et al. Activation of the α7-Nicotinic acetylcholine receptor reverses complete freund adjuvant-induced mechanical hyperalgesia in the rat via a central site of action. Journal of Pain. 2008;9(7):580–7.
54. Fehrenbacher JC, Vasko MR, Duarte DB. Models of inflammation: carrageenan- or Complete Freund's Adjuvant (CFA)-induced edema and hypersensitivity in the rat. Curr Protoc Pharmacol. 2012;56(1):5.4.1–54.
55. AlSharari SD, Freitas K, Damaj MI. Functional role of alpha7 nicotinic receptor in chronic neuropathic and inflammatory pain: Studies in transgenic mice. Biochem Pharmacol. 2013;86(8):1201–7.
56. Pabst M, Braganza O, Dannenberg H, Hu W, Pothmann L, Rosen J, et al. Astrocyte Intermediaries of Septal Cholinergic Modulation in the Hippocampus. Neuron. 2016;90(4):853–65.
57. Rosen SF, Ham B, Drouin S, Boachie N, Chabot-Dore AJ, Austin JS, et al. T-cell mediation of pregnancy analgesia affecting chronic pain in mice. J Neurosci. 2017;37(41):9819–27.
58. Mogil JS. Qualitative sex differences in pain processing: emerging evidence of a biased literature. Nat Rev Neurosci. 2020;21(7):353–65.
59. Chillingworth NL, Morham SG, Donaldson LF. Sex differences in inflammation and inflammatory pain in cyclooxygenase-deficient mice. Am J Physiol Regul Integr Comp Physiol. 2006;291(2):R327–34.
60. Mapplebeck JC, Beggs S, Salter MW. Molecules in pain and sex: a developing story. Mol Brain. 2017;10(1):9.
61. Rojas-Colon LA, Dash PK, Morales-Vias FA, Lebron-Davila M, Ferchmin PA, Redell JB, et al. 4R-cembranoid confers neuroprotection against LPS-induced hippocampal inflammation in mice. J Neuroinflammation. 2021;18(1):95.
62. Naser PV, Kuner R. Molecular, cellular and circuit basis of cholinergic modulation of pain. Neuroscience. 2018;387:135–48.
63. Bagdas D, Gurun MS, Flood P, Papke RL, Damaj MI. New insights on neuronal nicotinic acetylcholine receptors as targets for pain and inflammation: a focus on alpha7 nAChRs. Curr Neuropharmacol. 2018;16(4):415–25.
64. Lee RH, Vazquez G. Activation of alpha 7 nicotinic acetylcholine receptor protects M2 macrophages from ER stress-induced apoptosis. Faseb J. 2013;27(S1):884.1.
65. Chan TW, Langness S, Cohen O, Eliceiri BP, Baird A, Costantini TW. CHRFAM7A reduces monocyte/macrophage migration and colony formation in vitro. Inflamm Res. 2020;69(7):631–3.
66. Baez-Pagan CA, Delgado-Velez M, Lasalde-Dominicci JA. Activation of the macrophage alpha 7 nicotinic acetylcholine receptor and control of inflammation. J Neuroimmune Pharmacol. 2015;10(3):468–76.
67. Francis-Malave AM, Gonzalez SM, Pichardo C, Wilson TD, Rivera-Garcia LG, Brinster LR, et al. Sex differences in pain-related behaviors and clinical progression of disease in mouse models of colonic pain. Pain. 2022;164(1):197–215.
68. Velez-Carrasco W, Green CE, Catz P, Furimsky A, O'Loughlin K, Eterovic VA, et al. Pharmacokinetics and Metabolism of 4R-Cembranoid. PLoS One. 2015;10(3):e0121540.
69. Compton WM, Volkow ND. Major increases in opioid analgesic abuse in the United States: Concerns and strategies. Drug Alcohol Depend. 2006;81(2):103–7.
70. Picciotto MR, Kenny PJ. Mechanisms of Nicotine Addiction. Cold Spring Harb Perspect Med. 2021;11(5):a039610.
71. Wilkerson JL, Deba F, Crowley ML, Hamouda AK, McMahon LR. Advances in the In vitro and In vivo pharmacology of Alpha4beta2 nicotinic receptor positive allosteric modulators. Neuropharmacology. 2020;168:108008.
72. Pagán OR, Rowlands AL, Fattore AL, Coudron T, Urban KR, Bidja AH, et al. A cembranoid from tobacco prevents the expression of nicotine-induced withdrawal behavior in planarian worms. Eur J Pharmacol. 2009;615(1–3):118–24.
73. Freitas K, Ghosh S, Ivy Carroll F, Lichtman AH, Imad DM. Effects of alpha7 positive allosteric modulators in murine inflammatory and chronic neuropathic pain models. Neuropharmacology. 2013;65:156–64.
74. Munro G, Hansen R, Erichsen H, Timmermann D, Christensen J, Hansen H. The alpha7 nicotinic ACh receptor agonist compound B and positive allosteric modulator PNU-120596 both alleviate inflammatory hyperalgesia and cytokine release in the rat. Br J Pharmacol. 2012;167(2):421–35.
75. Mogil JS. Qualitative sex differences in pain processing: emerging evidence of a biased literature. Nat Rev Neurosci. 2020;21(7):353–65.
76. Ghasemlou N, Chiu IM, Julien JP, Woolf CJ. CD11b+Ly6G- myeloid cells mediate mechanical inflammatory pain hypersensitivity. Proc Natl Acad Sci U S A. 2015;112(49):E6808–17.
77. Shi L, Xu H, Wu Y, Li X, Zou L, Gao J, Chen H. Alpha7-nicotinic acetylcholine receptors involve the imidacloprid-induced inhibition of IgE-mediated rat and human mast cell activation. RSC Adv. 2017;7:51896–906.
78. Gu S, Knowland D, Matta JA, O'Carroll ML, Davini WB, Dhara M, et al. Hair cell alpha9alpha10 nicotinic acetylcholine receptor functional expression regulated by ligand binding and deafness gene products. Proc Natl Acad Sci U S A. 2020;117(39):24534–44.

79. Wang Y, Pereira EF, Maus AD, Ostlie NS, Navaneetham D, Lei S, et al. Human bronchial epithelial and endothelial cells express alpha7 nicotinic acetylcholine receptors. Mol Pharmacol. 2001;60(6):1201–9.
80. Palma E, Bertrand S, Binzoni T, Bertrand D. Neuronal nicotinic alpha 7 receptor expressed in Xenopus oocytes presents five putative binding sites for methyllycaconitine. J Physiol. 1996;491(Pt 1):151–61.
81. Puchacz E, Buisson B, Bertrand D, Lukas RJ. Functional expression of nicotinic acetylcholine receptors containing rat alpha 7 subunits in human SH-SY5Y neuroblastoma cells. FEBS Lett. 1994;354(2):155–9.
82. Halder N, Lal G. Cholinergic System and Its Therapeutic Importance in Inflammation and Autoimmunity. Front Immunol. 2021;12:660342.
83. Sabeva NPO, Ferrer-Acosta Y, Eterovíc V, Ferchmin P. In vivo evaluation of the acute systemic toxicity of (1S,2E,4R,6R,7E,11E)-Cembratriene-4,6-diol (4R) in sprague dawley rats. Nutraceuticals. 2022;2(2):60–70.

Publisher's Note